Kristian Gavric, BSc

Development of a Continuous Chemo-Enzymatic Two-Step Synthesis of Resveratrol Derivatives

MASTER'S THESIS

to achieve the university degree of

Diplom-Ingenieur

Master's degree program: Verfahrenstechnik

submitted to

Graz University of Technology

Supervisors:

Assoc.Prof. Dipl.-Ing. Dr.techn Gruber-Wölfler Heidrun

Dipl.-Ing. Bianca Grabner BSc

Institute of Process and Particle Engineering

Graz, January 2020

"Science without religion is lame,

religion without science is blind."

- Albert Einstein

STATUTORY DECLARATION

I declare that I have authored this thesis independently, that I have not used other than the declared sources / resources, and that I have explicitly marked all material which has been quoted either literally or by content from the used sources. The text document uploaded to TUGRAZonline is identical to the present master's thesis.

Acknowledgement

I would like to thank the Institute of Process and Particle Engineering, especially Prof. Gruber-Wölfler and Prof. Khinast for giving me the opportunity to conduct my master thesis at their institute.

A big thank you goes to my supervisor Bianca Grabner! She was always a great support throughout my work. All this was only possible due to her input and advice at all times but also her willingness to listen to my own ideas. Thanks to Bianca, I learned a lot about scientific working, chemistry and research in general.

Further, I thank all CoSy-Bros and all the other members of the institute for the last one and a half years I spent there during my study. It was always a pleasure to work with them in a friendly and relaxed working atmosphere and I especially enjoyed the coffee and lunch breaks and all the other activities we had together.

At the end, I would like to give a huge thank you to my girlfriend Nikolina, my family, friends and my guys from the football club for their love and support during the past few years. Without them none of this would be possible!

Abstract

In the framework of the present master thesis a fully integrated chemo-enzymatic process for the synthesis of resveratrol derivatives was developed. The reaction sequence comprises an enzymatic decarboxylation of phenolic acids by immobilized phenolic acid decarboxylase from *Bacillus subtilis* (*Bs*PAD) in alginate beads in the first step and a heterogeneous Heck coupling reaction with an aryl halide by a supported palladium catalyst ($Ce_{0.20}Sn_{0.79}Pd_{0.01}O_{2-\delta}$) in a subsequent step. Using deep eutectic solvents as part of a sophisticated solvent mixture, solubility problems of the reactants were solved and, additionally, a higher reaction temperature was accessible. Several reaction parameters were optimized in batch and two continuous flow approaches including the application of a 3D-printed continuous stirred tank reactor (CSTR) followed by a fixed bed reactor and a series of two packed bed reactors were developed. The latter allowed operation of the continuous synthesis for up to 24 h with several different derivatives as starting material. Depending on the utilized setup, overall yields of about 25 % were achieved. Furthermore, the flexible construction allows processing of the substrates in form of solutions with concentrations up to 20 mmol/l and suspensions with loadings up to 45 mmol/l.

In addition, a catalytic rearrangement reaction of 4-(1-phenylvinyl) phenol (side product of the reaction sequence) to 4-hydroxystilbene (targeted product of the reaction sequence) caused by migration of a phenyl group was discovered. The reaction occurs in presence of palladium as catalyst under basic conditions. Consequently, this seems to be a method to further enhance the yield and selectivity of the reaction cascade.

Parts of the results of this work are published by Grabner *et al*[1].

Kurzfassung

Im Rahmen der vorliegenden Masterarbeit wurde ein vollständig integrierter chemo-enzymatischer Prozess zur Synthese von Resveratrol-Derivaten entwickelt. Die Reaktionssequenz beinhaltet eine enzymatische Decarboxylierung von Phenolsäuren mittels immobilisierter Phenolsäure-decarboxylase vom *Bacillus subtilis* (*Bs*PAD) in Alginatgelpartikel im ersten Schritt und eine heterogene Heck-Kupplung mit Arylhaliden mittels eines festen Palladiumkatalysator ($Ce_{0.20}Sn_{0.79}Pd_{0.01}O_{2-\delta}$) im darauffolgenden Schritt. Durch Verwendung von stark eutektischen Lösungsmitteln als Bestandteil einer ausgefeilten Lösungsmittelmischung, konnten Probleme mit der Löslichkeit der Reaktanten gelöst werden und zusätzlich wurde eine höhere Reaktionstemperatur ermöglicht. Mehrere Reaktionsparameter wurden in Batch optimiert und zwei kontinuierliche Ansätze wurden entwickelt, die einen 3D-gedruckten kontinuierlichen Rührkesselreaktor (CSTR) gefolgt von einem Festbettreaktor und eine Serie von Festbettreaktoren beinhalten. Letzterer ermöglichte die kontinuierliche Synthese für bis zu 24 h mit einer Reihe an Substratderivaten zu betreiben. Abhängig vom verwendeten Aufbau konnten Gesamtausbeuten von bis zu 25 % erreicht werden. Weiters erlaubt die flexible Konstruktion das Zuführen der Substrate in Form von Lösungen mit Konzentrationen bis zu 20 mmol/l oder Suspensionen mit Beladungen bis zu 45 mmol/l.

Zusätzlich wurde eine katalytische Umlagerung von 4-(1-Phenylvinyl) phenol (Nebenprodukt der Reaktionssequenz) zu 4-Hydroxystilben (Zielprodukt der Reaktionssequenz), verursacht durch Wanderung einer Phenylgruppe, entdeckt. Die Reaktion tritt in Anwesenheit von Palladium als Katalysator unter basischen Bedingungen auf. Damit scheint dies eine Methode zur weiteren Verbesserung der Produktausbeute und Selektivität der Reaktionsfolge zu sein.

Teile der Ergebnisse dieser Arbeit wurden von Grabner *et al*[1] publiziert.

Contents

1   Motivation

There is growing interest in resveratrol and its derivatives for medical application in recent years as it turns out that the naturally occurring stilbenes have excellent anti-oxidative, anti-inflammatory, antidiabetic and antiaging properties.[2,3]

The aim of this work was to develop a fully integrated two-step continuous process for the synthesis of resveratrol derivatives **4aa'-4eb'** (Scheme 1). The first step is an enzymatic decarboxylation of substituted *trans*-coumaric acids **1a-1e** using phenolic acid decarboxylase from *Bacillus subtilis* (*Bs*PAD). As solvent a mixture of potassium phosphate (KPi) buffer and deep eutectic solvent (DES) was used. DES was introduced to enhance the solubility of the substrates. Further, the formed 4-vinylphenol derivatives **2a-2e** are linked with iodobenzene **3a'** or 4-iodophenol **3b'** in a palladium-catalyzed Heck cross-coupling reaction, giving the targeted resveratrol derivatives. In this second step, again DES is used to overcome solubility issues of the educts. **5aa'-5eb'** occur as side products of the Heck reaction. In this work, the reaction parameters should be adjusted in a way to maximize the formation of the main product while also reducing the amount of the side product.
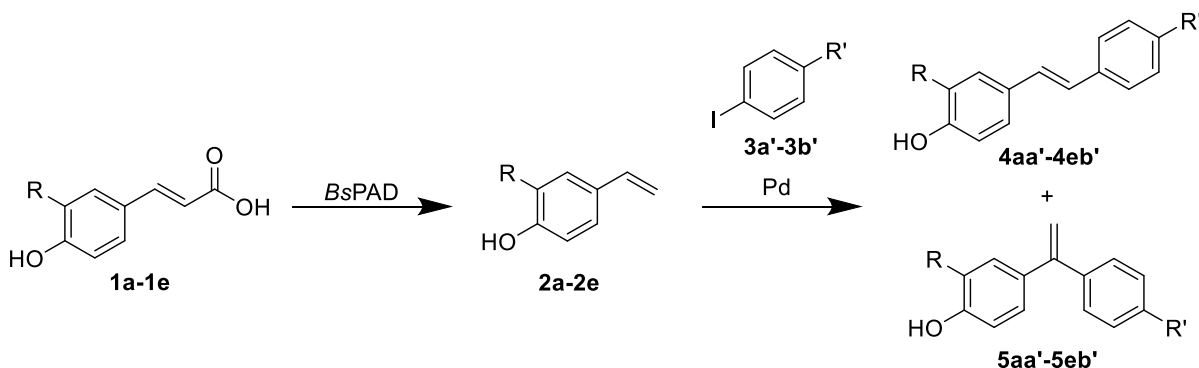

a: R = H   a': R = H
b: R = OMe   b': R = OH
c: R = F
d: R = Cl
e: R = Br

Scheme 1. Overview of substrates and the performed two-step syntheses of different resveratrol derivatives.
First step enzymatic decarboxylation, second step palladium-catalyzed Heck coupling.
*Bs*PAD = phenolic acid decarboxylase (*Bacillus subtilis*)

2 Introduction

2.1 Resveratrol and derivatives

The targeted products of this thesis are stilbenes, diarylethenes, derivatives of which attracted a lot of attention in the past decade, especially in the fields of pharmacy and medicine. The most important representative of this substance class is resveratrol (*E*- 3,5,4'- trihydroxystilbene, see Scheme 2), a natural product that is found in various plants and fruits, but above all in grapes.
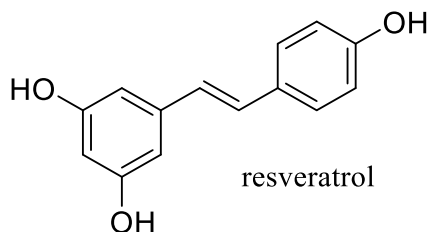
Scheme 2. Molecular structure of resveratrol (*E*- 3,5,4'- trihydroxystilbene)

Resveratrol was first isolated from roots of white hellebore (*Veratrum grandilflorum O. Loes*) in 1940.[4] Ever since, resveratrol and its derivatives[2,3] became important ingredients of many medical applications for prevention of and cure for a variety of diseases. In the following, some of the indication areas are listed to demonstrate the diverse potential of resveratrol and its derivatives as active pharmaceutical ingredients (API):

Cancer[5–8]
  – Prostate
  – Breast
  – Colorectal

Cardiovascular diseases[8,9]
  – Coronary artery disease
  – Atherosclerosis
  – Hypertension
  – Oxidative Stress

Non-alcoholic fatty liver disease[12]

Neurological disorders[9,10]
  – Alzheimer's disease
  – Ischemic stroke

Diabetes[9,11,12]
  – Type 2
  – Impaired Glucose Tolerance

Obesity[13]

Besides all these impressive medical applications, resveratrol is also topic of other branches of research and industry. For example, in early 2019 Stokes *et al.*[14] patented a "process for making a container with a resveratrol layer", where they use an inner coating including resveratrol to enhance the shelf life of beverage (especially wine).

As naturally occurring substances, resveratrol and its derivatives are mostly obtained from the extraction of grapes and other plants. Nevertheless, there are a few possible chemical and biochemical synthesis routes, including for instance, Perkin reactions[15], metal catalyzed decarboxylation[15] or, like in this work, a Heck cross-coupling reaction. The obtained resveratrol can then be used in further reaction steps to synthesize different derivatives and oligomers[16,17], which are applied as API as mentioned before.

2.2   Heck reaction

In this thesis, resveratrol derivatives were synthesized using Heck reaction or Heck coupling, which is a palladium catalyzed C-C cross-coupling of vinyl components (in this work vinylphenol derivatives) and aryl halides. It was first described by Richard Fred Heck in 1972.[18] R.F. Heck was honored with the Nobel Prize in Chemistry with E. Negishi and A. Suzuki for their achievements in the field of "palladium-catalyzed cross couplings in organic synthesis" in 2010.[19]

Despite the Heck reaction being a well-known and important reaction in organic chemistry, the exact reaction mechanism (especially the role of different occurring Pd species) is still a debated topic nowadays. In Scheme 3 a reaction mechanism proposed by Biffis *et al.*[20] for a homogeneous Heck reaction is shown. The reason, why a homogeneous instead of a heterogeneous reaction mechanism is described in this section, even though in this thesis a heterogeneous approach was used, will become apparent shortly. At the reaction onset, solid Pd(0) undergoes an oxidative addition of aryl halide ArX, where X = I, Br, Cl or OTf (= $CF_3SO_3^-$; triflate or trifluoromethanesulfonate, technically not a halide but often mentioned alongside the other real halides for this reaction). This process activates the C-atom of the aryl by increasing its electronegativity. In the next step, the vinyl component is reversibly added to [Ar-Pd-X], resulting in a so-called π-complex. After a reversible migration of the aryl, a covalent bond between the palladium and the vinyl C-atom is formed. This compound is also known as σ-intermediate. The subsequent reaction step is another reversible formation of a π-complex as a result of the separation

of the desired coupling product from the intermediate. After the reductive elimination of the product and HX, dissolved Pd(0) is released. This species can immediately be recycled in the catalytic process by another oxidative addition of ArX and the reaction starts all over again. Biffis and co-workers call this instant recycling a "homogeneous shunt". Besides this traditional mechanism, they stated that Pd(0) could agglomerate and form Pd colloids (nanoparticles), "if this process is not too slow in comparison to the homogeneous shunt".[20] These colloids are also capable of acting as catalytically active species and are oxidized by ArX as well. Hence, the particles are further involved in the cyclic reaction mechanism. However, further agglomeration of the colloids results in larger particles until they eventually create less active Pd black and in this way steadily contribute to the inactivation of the palladium catalyst.
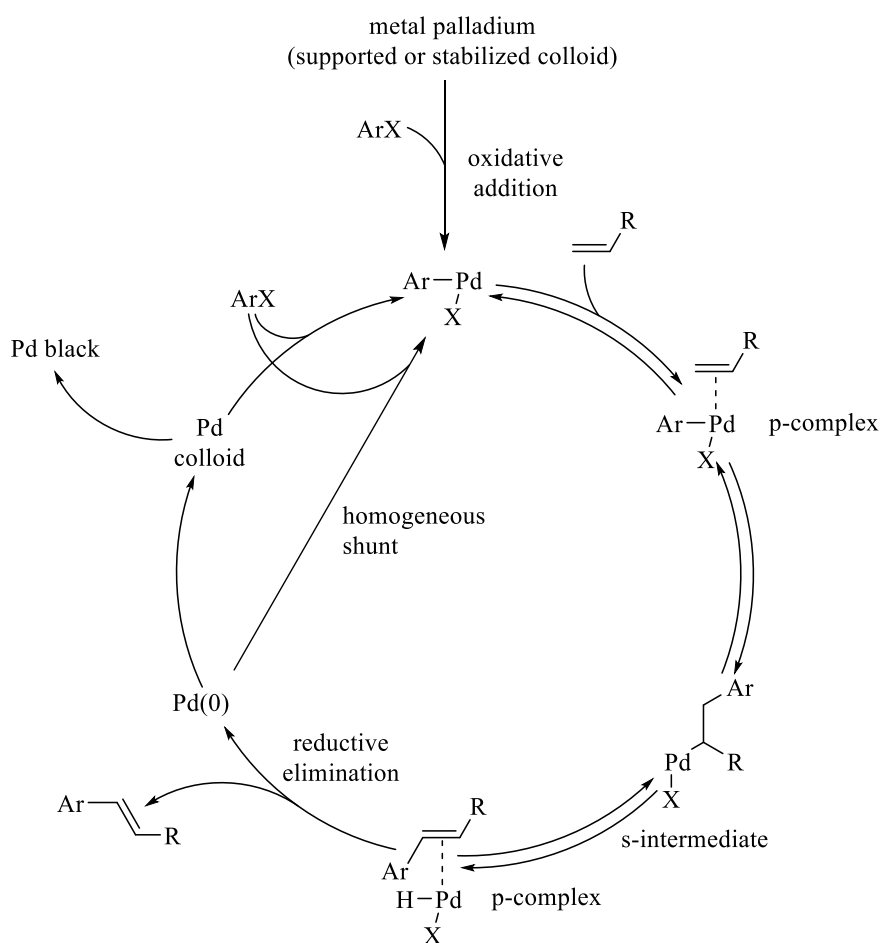
Scheme 3. Proposed reaction mechanism of the homogeneous Heck coupling by Biffis *et al.*[20]. The cyclic reaction process starts with the oxidative addition followed by the formation of the π-complex and σ-intermediate. After the elimination of the coupling product Pd(0) is released, which either immediately reacts with another aryl halide or form palladium colloids (nanoparticles). These particles can also enter the reaction cycle or further agglomerate and form Pd black. Reproduced from [20] and [21].

In the shown mechanism, palladium acts as homogeneous catalyst in solution. However, the palladium is introduced as supported metal or stabilized colloid, which means the application of a heterogeneous metallic catalyst. Biffis *et al.*[22] explained in another review in 2018 why the reaction mechanism should not be described as a heterogeneous reaction, e.g. as surface reaction. The point is that the introduced catalyst only serves as pre-catalyst or source of palladium, which dissolves while undergoing the oxidative addition of ArX and in this way starts the cyclic reaction mechanism. This "pseudo-heterogeneous" behavior was confirmed in many works in the last decade, e.g. by Schmidt *et al.*[23,24], Huang *et al.*[25], Reimann *et al.*[26] and Pryjomska-Ray *et. al.*[27] to just name a few. In Scheme 4 the different palladium species involved in the Heck reaction and their interaction with each other are shown, as described by Schmidt and co-workers[23]. All the zerovalent species, $Pd(0)_{dissolved}$, $Pd_{colloid}$ (nanoparticles) and $Pd_{heterogen}$ (larger metal particles) are contributing to the formation of Pd(II) via oxidative addition of ArX. Each of these types can be found simultaneously, no matter what pre-catalyst or support is chosen.[25,26] At the end of the reaction and after the reductive elimination of the Heck product and HX, again Pd(0) is formed. This dissolved palladium can re-enter the reaction cycle immediately or agglomerate and grow to form larger particles, like mentioned before. The problem with the occurrence of multiple species is that the reliability of heterogeneity tests, such as hot-filtration test and poisoning with mercury become questionable because of the different effects of the methods on the individual species and the complicated interactions (dissolution rate, aggregation rate, adsorption, …) between them.[24] Consequently, there are doubts if a pure heterogeneous Heck reaction with palladium even exists.[22,24] Also, Cantillo and Kappe pointed out in their review in 2014[28] that "significant leaching of the transition metal out of the packed-bed catalyst will almost inevitably occur". Thus, the question for heterogeneous continuous flow reactions is not if the catalyst is leaching but rather "how much". The heterogeneous catalyst used in this work was Pd supported by a cerium-tin-oxide with the general formula $Ce_{0.99-x}Sn_xPd_{0.01}O_{2-\delta}$. More details on the catalysts in section 3.1 and 4.5, respectively.
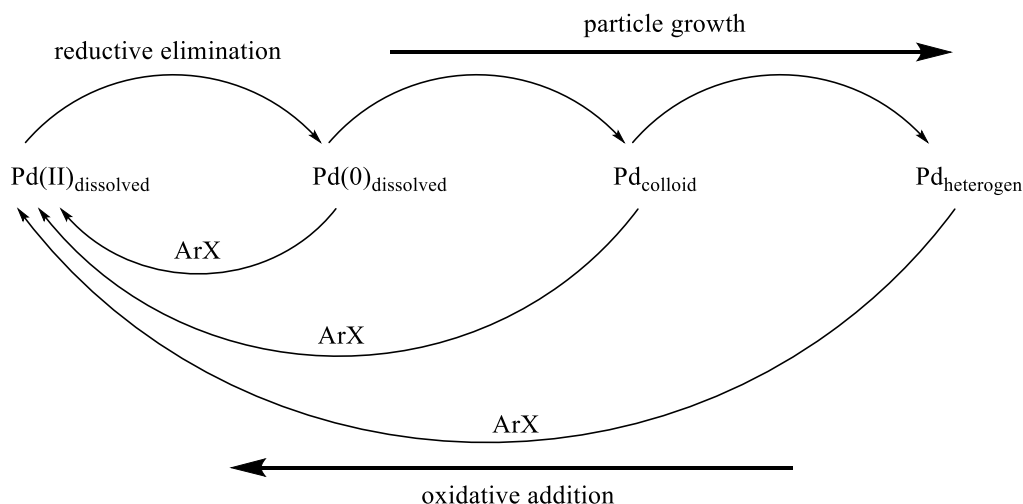
Scheme 4. Illustration how all different species of palladium, namely $Pd(II)_{dissolved}$, $Pd(0)_{dissolved}$, $Pd_{colloid}$ (nanoparticles) and $Pd_{heterogen}$ (metal particles), interact in the mechanism of the Heck reaction. This cycle of particle growth and palladium dissolution due to the oxidative reduction by ArX takes places alongside the original reaction mechanism in Scheme 3 and gives a better understanding of the nature the Heck reaction. Reproduced from [23]

2.3   Enzymatic decarboxylation of phenolic acids

A sustainable source of vinylphenol derivatives for the Heck coupling are naturally occurring phenolic acids, such as cinnamic acid, *p*-coumaric acid or caffeic acid.[29] The desired vinyl compounds are obtained after decarboxylation of these acids by a phenolic acid decarboxylase (PAD), an enzyme produced by several bacteria[30] and fungi[31]. Due to the wide distribution of the acids and the enzyme, the products of these decarboxylation reactions are found in various foods, e.g. cinnamon, coffee and beer.[32] Although styrene (vinylbenzene) and similar substances are unwanted ingredients in our food and may also be harmful to humans[32,33], these chemicals are highly relevant as raw materials throughout chemistry.

In this work, PAD from *Bacillus subtilis* (*Bs*PAD) was used for the decarboxylation of *p*-coumaric acid and several derivatives. Scheme 5 shows an overview of the reaction mechanism proposed by Rodriguez *et al.*[34]. The substrate enters the enzymes active site and binds to the hydroxy groups of two tyrosine molecules (Tyr_{18}, Tyr_{20}) with its carboxylate group by forming polar hydrogen bonds. At the other end of the substrate molecule, the *p*-hydroxy group, the reaction is induced by the catalytic part of the enzyme, glutamic acid (Glu_{71}). A quinone methide intermediate is formed,

which in the next step is transformed to 4-vinylphenol by elimination of the carboxyl group and the release of CO_2.
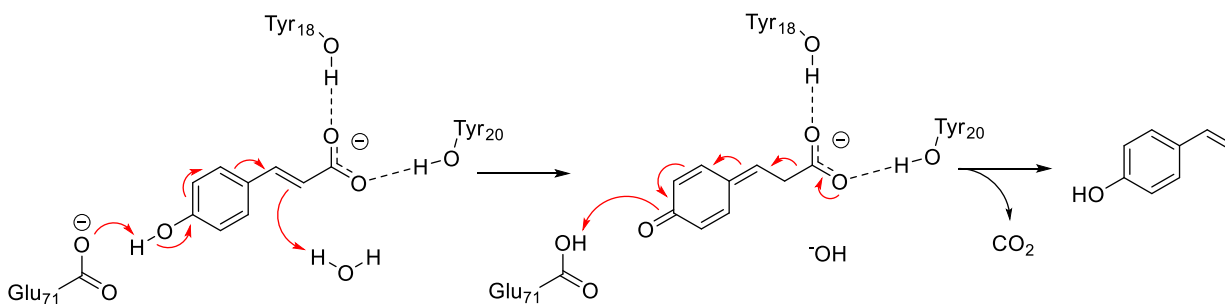
Scheme 5. Mechanism of the enzymatic decarboxylation of *p*-coumaric acid by *Bs*PAD. Reproduced from [34].

2.4   Enzyme immobilization

In this work, the decarboxylation step should be carried out in a heterogeneous reaction, thus the water soluble *Bs*PAD needs to be immobilized. Numerous procedures for the immobilization of enzymes are described in literature and are categorized in two groups, namely irreversible and reversible methods. Irreversible methods are for example the connection of the enzyme to a supporting structure with covalent bonds, the entrapment in beads of fibers, microencapsulation or cross-linking of enzyme molecules to clusters. The reversible methods include non-covalent binding forms, such as adsorption, ionic binding, chelation, and others. Each method has its pros and cons, so the method has to be chosen individually for every application after consideration of different parameters, such as hydrophilicity, inertness of support towards enzyme, biocompatibility, costs, and others.[35,36]

The encapsulation of *Bs*PAD in alginate beads was chosen as immobilization method for the application in continuous flow. The most important advantages of this approach are the simple and fast preparation of the beads, low toxicity and the low costs of the applied materials. Also, this way of immobilization turned out to be very well suitable for the used reaction system and allowed to obtain satisfying results.

Alginate is a naturally occurring polysaccharide consisting of residues of α-L-guluronic acid (G) and β-D-mannuronic acid (M) and is mostly used as dry sodium alginate powder. The monomers are connected in a random order and this leads to the formation of three different monomer-sequences, namely GM/MG-, G- or M-blocks, as illustrated in Scheme 6 (A). These blocks

comprise different amounts of monomers, so the length of the blocks varies and influences the rheological properties[37] of the network formed by the integration of divalent metal cations, e.g. Ba^{2+} or Ca^{2+} (see Scheme 6 (B)).[38] The emerging stable polymer structure is used to immobilize enzymes by entrapping them inside the network while also allowing permeation of smaller sized molecules, such as buffers, substrates and products.
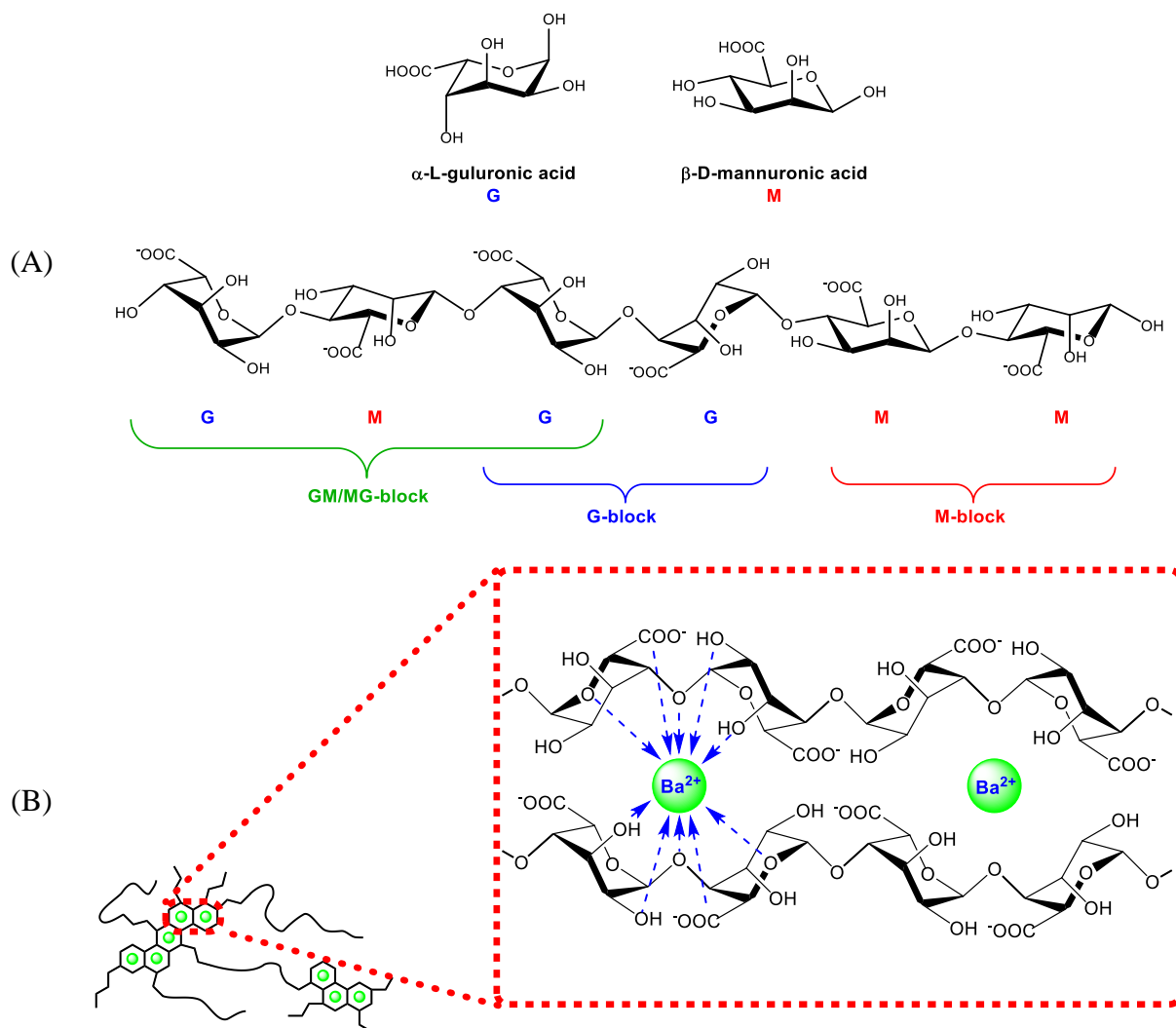
Scheme 6. (A) alginate monomers α-L-guluronic acid (G) and β-D-mannuronic acid (M) and the possible polymer configurations which are categorized in GM/MG-, G- and M-blocks. The blocks appear in different lengths (amount of monomers) and are arranged in random order.
(B) Schematic depiction of alginate polymer surrounding Ba^{2+} ions. In the close-up a G-block and its interactions with a Ba^{2+} ion are shown. Also GM/MG- and M-blocks are capable of binding to the metal ion as shown. Reproduced from [38].

2.5 Flow chemistry

The two-step synthesis of resveratrol derivatives was conducted in an integrated continuous flow setup. This allows to overcome problems such as the high reactivity of the intermediate vinyl compound and thus lowers material losses (compared to a batch synthesis with purification of the products between the individual reaction steps). Nowadays, continuous flow processes are becoming increasingly important in pharmaceutical manufacturing and chemistry. The main benefits of flow chemistry compared to batch are found in terms of safety, environment, economy and alternative synthesis routes. For instance, with the usually small channel sizes of flow reactors, a high surface to volume ratio is achieved in comparison to batch processes with the same throughput. This allows a fast heat transfer from/to a surrounding heating or cooling medium and in that way highly endo/-exothermic reactions are much easier to control. Unlike in batch synthesis, there is no emptying, cleaning and refilling procedure, what leads to lower exposure to humans and nature hazardous materials. Another advantage of continuous manufacturing is the lack of dead-times. As a result, high amounts of energy, time and waste can be saved but also automation and a constant product quality become possible. Moreover, numerous new chemical reactions and synthesis routes are accessible with the application of continuous flow microreactors. In the past few years, various examples of reactions with hazardous substances and highly exothermic or high-pressure reactions were successfully performed in flow.[39,40] Also, new approaches with multi-phase reactions, photo- or electrochemistry and catalytic reactions were developed[39,41–43], which surpass the possibilities of batch synthesis by far. With all these new opportunities and benefits, continuous manufacturing is often associated with green chemistry and generally considered a more sustainable way of chemical processing than traditional batch procedures.[44,45]

2.6 Integrated chemo-enzymatic flow setups

The application of sequential biocatalytic and metal catalyzed reactions is a forward-looking subject in today's chemistry. Combining the selectivity of enzymes with the widespread possibilities of metal-catalysis opens a whole field of new synthesis routes and together with the use of continuous process technologies this topic became very interesting and promising in recent years.

Exciting examples of chemo-enzymatic syntheses in flow performed in the past few years are shown in Scheme 7. The first reaction sequence in Scheme 7 (a) was conducted by Sperl *et al.*[46] and starts with gold-catalyzed oxidation of a carbohydrate. They then used a continuous filter module to separate the intermediate sugar acid anion, which is dehydrated in the next step by an enzyme. The obtained product 2-keto-3-deoxy sugar acid is then purified by continuous ion exchange chromatography. Scheme 7 (b) shows a dynamic kinetic resolution of amines by Faraks *et al.*[47] In the first step a racemic mixture of an amine undergoes a selective enzyme catalyzed *N*-acetylation in column A where the desired (*R*)-product is synthesized. In column B a simultaneous racemization of unreacted substrate and *N*-acetylation of the product takes place. The unreacted (*S*)-amine from the outlet of the first step is racemized by a supported palladium catalyst, while the emerging (*R*)-amine is immediately converted by the enzyme. In this way a yield close to 100 % of the (*R*)-product is possible instead of only 50 % without the racemization step. Another chemo-enzymatic flow reaction was reported by Peng *et al.*[48] (see Scheme 7 (c)). They used an enzymatic decarboxylation of *p*-coumaric acid to synthesize 4-vinylphenol which was then further converted in a Heck reaction to obtain 4-hydroxystilbene. This reaction sequence is also in the scope of this thesis. As shown in the scheme, Peng and co-workers used 2-hydroxyethyl agarose to immobilize the enzyme. Using a 3D-printer they created modules of the agarose network which are utilized as fixed bed in the flow reactor. The following Heck reaction is performed in batch and an overall yield of about 15 % was achieved.
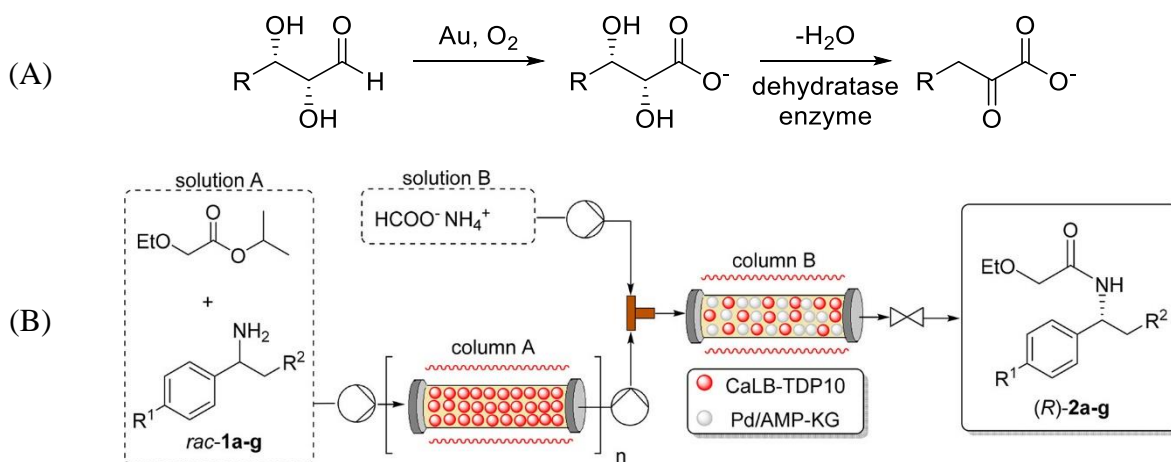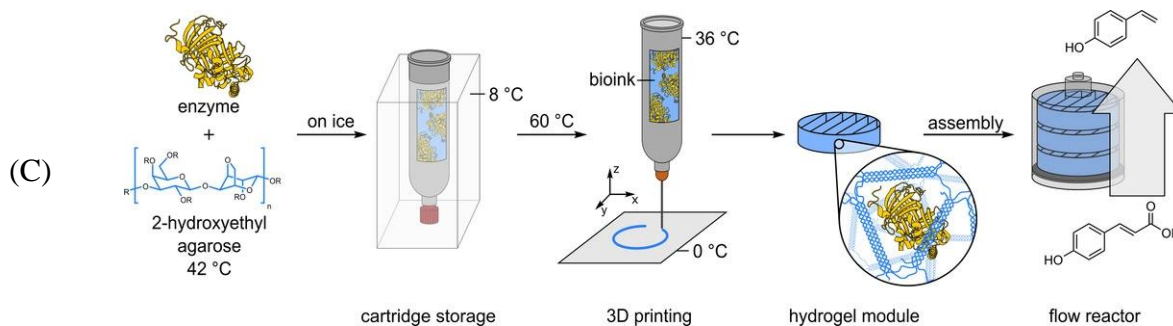
Scheme 7. Examples for chemo-enzymatic continuous flow reactions.
(A) Gold-catalyzed oxidation of carbohydrates with subsequent enzymatic dehydration to form 2-keto-3-deoxy sugar acids by Sperl *et al.*[46]
(B) Chemo-enzymatic dynamic kinetic resolution of amines by Farkas *et al.* CaLB-TDP10 = lipase (enzyme); Pd/AMP-KG = supported palladium catalyst. Scheme taken from [47].
(C) Enzymatic decarboxylation with subsequent Heck reaction by Peng *et al.* Scheme taken from [48]

2.7 Deep eutectic solvents

Despite all the benefits, there are also new challenges that arise with combined continuous flow synthesis. In case of the setup described in this work, the major questions were, how to select a solvent compatible to the organic and inorganic reactants and how to obtain optimized reaction conditions in step two with the solvent mixture of step one. An answer for both questions was found in the application of deep eutectic solvents (DESs).

DESs are a relatively new form of solvents and were first mentioned at the beginning of the 21st century.[49,50] They are special types of ionic liquids and are described as eutectic mixtures of Lewis or Brønsted acids and bases with a low melting point.[51] One of the first representative of DESs is a mixture of choline chloride (ChCl) and urea. A molar ratio of ChCl:urea =1:2 (mol:mol) gives a DES with a freezing point T_f of 12 °C, which is drastically lower than the T_f of the pure substances (T_f (ChCl) = 303 °C; T_f (urea) = 134 °C)[52]. This large depression of the T_f is achieved by the complexation of the anion (in this case chloride) by hydrogen bond donators (HBD) or metal halides (in this case urea as HBD). Thus, the anion is stabilized and sterically hindered from forming crystal structures with the cation (in this case choline-cation). As a result, the lattice energy drops and the freezing/melting point decreases drastically.[51]

There are four different types of DESs, which are distinguished by their composition and physical properties. In Table 1 the different types are listed with the respective ingredients. Type I and Type II both consist of a quaternary ammonium salt (QAS) and a metal chloride, with the difference that the metal chloride in Type II can contain different metal species and is applied in

form of a hydrate. Type III is a mixture of pure organic substances and requires a QAS and an HBD. This type of DESs is the most often used and is usually a liquid comprised of ChCl and amines/amides (e.g urea), diols (e.g. glycerol) or acids/diacids (e.g. malonic acid). Type IV is the only kind of DES that does not include a QAS, but only consists of a metal chloride and an HBD. In this case the metal salts split into anionic and cationic species. The HBD then forms a complex with the cation, which again lowers the lattice energy. One example is the DES $ZnCl_2$/urea where $[ZnCl(urea)]^+$, $[ZnCl(urea)_2]^+$ and $[ZnCl(urea)_3]^+$ cations and $[ZnCl_3]^-$, $[Zn_2Cl_5]^-$ and $[Zn_3Cl_7]^-$ anions are formed.[51,52]

Table 1. Categorization of deep eutectic solvents (DESs) in four types.[51,52] QAS = quaternary ammonium salt; cat^+ = residual part of the QAS binding with the chloride; M = metal; HBD = hydrogen bond donator; R = organic rest; Z = active organic rest with the role of the HBD; x, y = stoichiometric factors

Type	Ingredients	General formula	Metals & Residuals
Type I	QAS + metal chloride	$cat^+ Cl^- + MCl_x$	M = Zn, Sn, Fe, Al, Ga, In
Type II	QAS + metal chloride hydrate	$cat^+ Cl^- + MCl_x \cdot yH_2O$	M = Cr, Co, Cu, Ni, Fe
Type III	QAS + HBD	$cat^+ Cl^- + RZ$	Z = $CONH_2$, OH, COOH
Type IV	metal chloride + HBD	$MCl_x + RZ = MCl_{x-1}^+ \cdot RZ + MCl_{x+1}^-$	M = Al, Zn Z = $CONH_2$, OH

Besides these synthetic types of DESs there are natural deep eutectic solvents (NADESs) appearing in nature. The NADESs consist of sugars, amines and organic acids (amino acids) and are synthesized by numerous plants and microorganisms. It was found that species living in harsh conditions (e.g. extreme cold or drought) are producing much higher contents of these NADES ingredients than those in milder regions. Thus, NADESs are presumably a key criterion for life in extreme environments.[53]

In the 21st century the application of DESs and ionic liquids increased greatly. Especially, DESs attracted the attention of research and industry because of the significant benefits that are accompanied by the novel solvent. Such advantages are that DESs are non-volatile, hardly

inflammable, less toxic than other ionic liquids and biodegradable which already makes them superior in comparison to other ionic liquids or usual organic solvents. Further, DESs have excellent solvent properties and are capable of dissolving inorganic metal salts and oxides (LiCl, CuO, …)[50,54] but also various organic components (alcohols, amines, proteins, cellulose, …)[55,56]. This way a wide range of applications emerged for DESs including the extraction of natural bioactive components[56], synthesis of biodiesel[54], biocatalysis[57], CO_2-capture[58], electrochemical applications[59] (possible due to high conductivity of DESs) and many others. All in all, DESs are perhaps the most powerful kind of green solvents and will definitely play a big role in the chemistry of the future.

3 Results and Discussion

3.1 Palladium catalysts – Performance of different catalyst types

One of the most important reaction parameters of every Heck coupling reaction is the applied palladium catalyst. The goal of this thesis was to develop a two-step reaction process including a palladium-catalyzed Heck reaction in continuous flow, which should be carried out with a heterogeneous palladium catalyst.

In order to find an appropriate catalyst, three different heterogeneous catalysts were tested. One of them is the so-called "Knitting Aryl Network Polymer" palladium catalyst (KAP-Pd). This catalyst consists of an organic support that allows immobilization of palladium atoms between triphenylphosphine groups. The alternatives were two metal oxide supported catalysts with dispersed palladium atoms in the crystal structure. The general formula of these catalysts is $Ce_{0.99-x}Sn_xPd_{0.01}O_{2-\delta}$, where x is 0.79 or 0.99, respectively. The catalysts are labeled according to their synthesis method SCM (Solution Combustion Method) as SCM-A (x = 0.79) and SCM-B (x = 0.99).

The catalysts were compared by performing a Heck reaction at identical conditions. **2a** (4-vinylphenol, 35.0 mol/l), **3a'** (iodobenzene, 52.5 mol/l, 1.50 mol eq. with respect to **2a**) and K_2CO_3 (52.5 mol/l) were dissolved in a solvent mixture of deep eutectic solvent (DES), aqueous potassium phosphate buffer (KPi-buffer), purified water and ethanol with the composition DES(A):KPi-buffer:H_2O:EtOH = 1:1:1:1 (v:v:v:v) (10 ml) and then heated to 85 °C (DES(A): ChCl:glycerol = 1:2 (mol:mol), see section 4.2). A reference sample (100 µl) was taken before adding the catalyst. The mass of catalyst was chosen in a way to keep the amount of palladium loading relative to the limiting substrate constant, which gave 13.5 mg of KAP-Pd and 12.7 mg of the SCM catalysts, respectively. At certain time points an aliquot of 100 µl was taken as sample and analyzed by HPLC (method B, see section 4.12).

Figure 1 shows the conversion X of **2a** and the yield Y of **4aa'** ((E)-4-styrylphenol) over time of the performed experiments. The reactions with KAP-Pd (red) and SCM-A (blue) gave almost identical courses of X and reached full conversion after a little more than 10 min. Also, the yield of both reactions develops similarly over time and reaching slightly more than 45 % after 240 min.

In contrast to that, the performance of the SCM-B catalyst was nowhere near the other two. In that reaction, the conversion did not exceed 20 % before 90 min of reaction time and only reached about 55 % at the end of the run. In addition to that, hardly any product was formed over the whole course of the experiment.
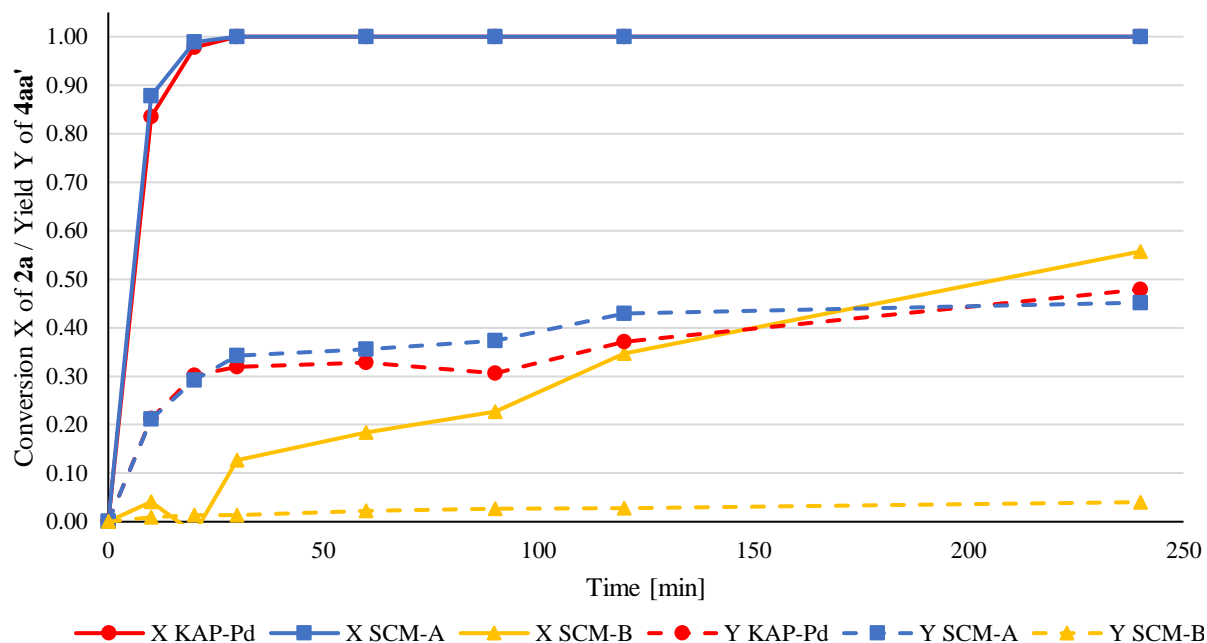

Figure 1. Catalyst comparison. Conversion X of **2a** (solid line) and yield Y of **4aa'** (dashed line) over time using different types of catalysts. Reaction temp.: 85 °C; **2a** (35.0 mmol/l); **3a'** and base in 1.50 mol eq. referring to **2a**; KAP-Pd (red): 13.5 mg; SCM-A (blue): 12.7 mg; SCM-B (yellow): 12.7 mg; DES(A):KPi-buffer:H$_2$O:EtOH = 1:1:1:1 (v:v:v:v) (10 ml)

KAP-Pd and SCM-A emerged to be most active in the chosen reaction system. In the next step, preliminary flow experiments were conducted to determine the performance of the catalysts in a packed bed reactor. Already in the early stage of the tests, it turned out that the applicability of the KAP-Pd in flow setups is limited. At the beginning of the flushing process at 85 °C, the outflow was a brownish solution and contained dissolved palladium. Consequently, the KAP-Pd is not useable for continuous reactions due to severe leaching. Conclusive evidence for the excessive leaching of palladium was brought by performing a batch reaction with the same procedure as described before for the comparison of the catalysts. Only this time 200 µl of the flushing solution (the volume was chosen randomly as the palladium concentration was not known) was added as catalyst. In Figure 2 the results of this reaction are shown, where the conversion of **2a** and the yield of **4aa'** over time is depicted. Without a doubt, high amounts of palladium leached out of the

packed bed reactor and therefore KAP-Pd was ruled out as possible catalyst. SCM-A performed much better in the preliminary flow experiment and met the requirements in terms of conversion and yield without significant leaching. As a result, catalyst SCM-A was used for most of the further batch and for all of the continuous flow reactions.
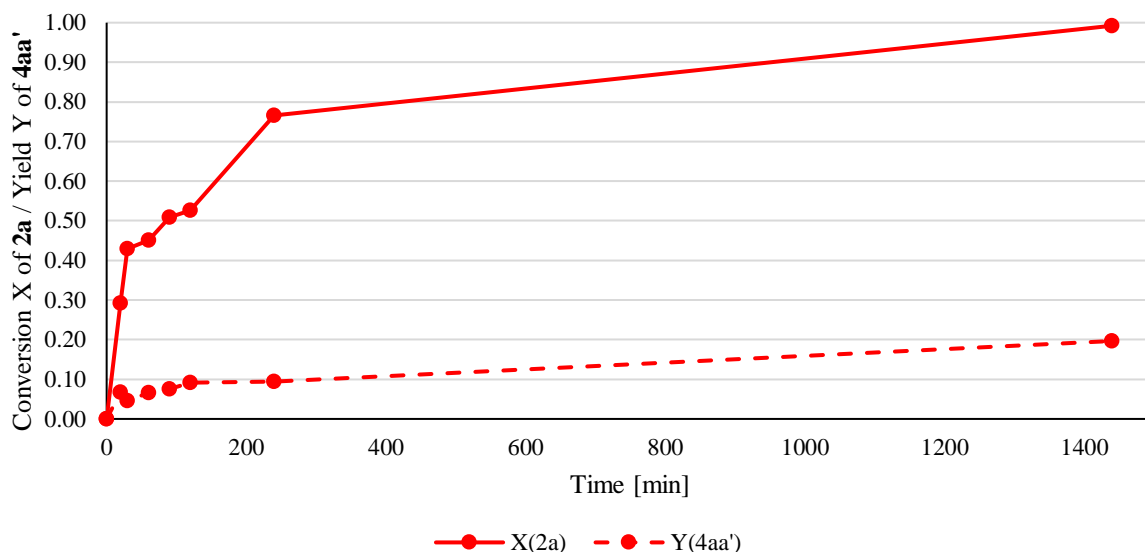

Figure 2. Conversion of **2a** and Yield of **4aa'** obtained using 200 µl of the flushing solution containing leached palladium form the preliminary flow experiment with KAP-Pd. Reaction temp.: 85 °C; **2a** (35.0 mmol/l); **3a'** and base in 1.50 mol eq. referring to **2a**; DES(A):KPi-buffer:H_2O:EtOH = 1:1:1:1 (v:v:v:v) (10 ml)

3.2   Reaction Temperature – Influence on Heck reactions

The reaction temperature is a crucial parameter for the determination of the optimal process conditions. Hence, the influence on the Heck coupling was investigated by performing the reaction at different temperatures. For this purpose, **2a** (10.0 mol/l, 1.10 mol eq., referring to **3a'**), **3a'** (9.1 mol/l) and K_2CO_3 (52.5 mol/l) were dissolved in DES(A):KPi-buffer:H_2O:EtOH = 6:5:2.25:6.75 (v:v:v:v) (10 ml) and heated to the required temperature. The composition of the used solvent corresponds to that one used in Heck reactions of combined flow setups (more on the background in section 3.4). After taking a reference sample (100 µl), the catalyst SCM-A (12.7 mg) was added. Samples (100 µl) were taken at different points in time and analyzed by HPLC (method B, see section 4.12).

In Figure 3 the influence of three different temperatures is shown by the conversion of **2a** over time in (A) and the HPLC peak area ratio of **4aa'** to **5aa'** in (B). As it was not possible to obtain a

proper calibration for the side product **5aa'**, only the peak areas given by the HPLC can be compared instead of the concentrations. However, the area ratio is sufficient to qualitatively assess the experimental results in terms of temperature dependency of the reaction.

As shown in Figure 3 (A) the conversion of the substrate was faster with higher temperatures, as expected. At 85 °C a conversion of about 70 % was reached after 5 min, whereas at 75 and 65 °C roughly half the conversion was observed within the same amount of time, respectively. A good performance at the beginning is of great importance, because of the short residence time in the continuous flow reactors in the intended final setup. Further, higher temperatures gave higher amounts of the desired product **4aa'** compared to the side product **5aa'**, as demonstrated by the area ratios in Figure 3 (B). All in all, the outcome of these experiments shows that the reaction temperature should be chosen as high as possible. Thus, additional reactions were performed at 90 °C, but it turned out that this temperature was too close to the boiling point of the solvent. Moreover, the solubility of CO_2 (formed by the decarboxylation reaction) decreases at higher temperatures. This would lead to problems in the continuous setup, as vapor and CO_2 bubbles disturb the flow of the liquid phase through the packed bed reactor. A consequence would be lower residence time, higher backmixing and severe losses in conversion and yield. For this reason, the temperature will be set to 85 °C for the Heck coupling reaction.

(A)   (B)
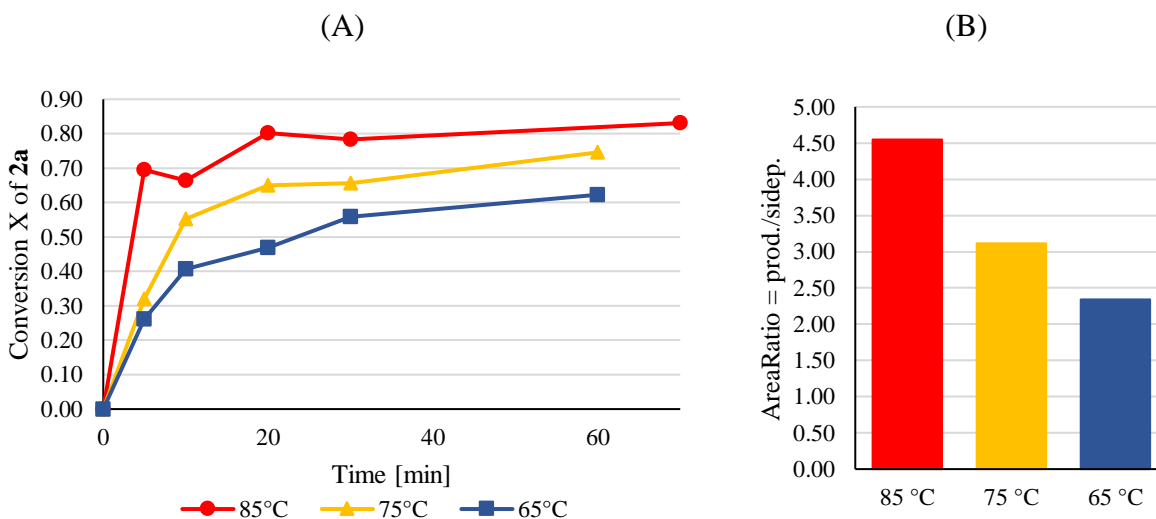
Figure 3. Influence of the reaction temperature on the performance of Heck reactions. **2a** (10.0 mmol/l); **3a'** (9.1 mmol/l); K_2CO_3 (52.5 mmol/l); SCM-A (12.7 mg); DES(A):KPi-buffer:H_2O:EtOH = 6:5:2.25:6.75 (v:v:v:v) (10 ml)
reaction temp.: red: 85 °C; yellow: 75 °C; blue: 65 °C
(A) Conversion of **2a** over time at different reaction temperatures
(B) HPLC area ratio of the desired product **4aa'** to the side product **5aa'** at different temperatures after 60 min reaction time

3.3 Selection of DES

The combination of two reaction steps in one flow setup is a big challenge due to numerous reasons. Particularly in this case, where an enzymatic step was combined with a metal catalytic reaction. Besides other difficulties, a major issue was the selection of a proper solvent system.

The enzymatic reaction requires an aqueous buffer with a pH of 6. In earlier works, Schweiger *et al.*[60] reported that the *Bs*PAD (phenolic acid decarboxylase form *Bacillus subtilis*) used for this reaction, shows an enhanced reaction performance in solvent mixtures of potassium phosphate buffer (KPi-buffer) and deep eutectic solvents (DES). The Heck reaction, on the other hand, is usually performed in a mixture of water and ethanol with basic pH, but as the final setup is a combined flow process, the Heck reaction had to be performed in a mixture of DES, buffer, water and ethanol. This already leads to complications, because the enzyme would precipitate in an ethanolic solution, the pH value had to be adjusted to specific values for each reaction and also the substrates for the decarboxylation and the reactants for the Heck coupling are hardly soluble in water.

In preliminary experiments, which were not scope of this work, a well performing solvent composition for the enzymatic step was found to be DES:KPi-buffer = 1:1 (v:v). The DES used for those tests was a mixture of choline chloride (ChCl):glycerol = 1:2 (mol:mol). In this work four different DES for the Heck reaction were investigated, which are summarized in Table 2. ChCl served as quaternary salt and was combined with of the hydrogen bond donors (HBD) glycerol, 1,2-propane diol, ethylene glycol or phenol in a ratio of 1:2 (mol:mol).

Table 2. Overview of used DES with ChCl as quaternary salt and different HBD. The molar ratio is set to salt:HBD = 1:2.

DES	quaternary salt	HBD
A		glycerol
B	ChCl	1,2-propane diol
C		ethylene glycol
D		phenol

It was found that all of the different DES can be applied for Heck reaction with even better results in terms of conversion and yield compared to water-ethanol solvents. One explanation for the

enhanced performance is the higher boiling point of the DES mixtures, thus the reaction can be conducted at higher temperatures. In preliminary tests, DES(A) gave the best results, which is particularly beneficial because this allows a good compatibility of the enzymatic decarboxylation and the subsequent Heck reaction in the flow experiments.

3.4 Solvent composition – Influence on Heck reactions

The further optimization of the solvent system was done with focus on the real conditions in the continuous setup. The final solvent composition was determined by two different stock solutions, one containing the substrate for the decarboxylation and the other containing an aryl iodide and base as reactants for the Heck coupling. The flow rates of both stocks are identical, meaning that the individual compositions of both stocks will contribute to equal parts. As mentioned before, the solvent for the enzymatic step is set to DES(A):KPi-buffer = 1:1 (v:v). Hence, only adjustments on stock 2 are possible, where the aryl iodide and the base have to be dissolved in an ethanol-water solution. It was difficult to obtain a stable solution of the reactants at room temperature because the high concentrations in the solution caused the mixture to split into two phases. This problem was avoided by simply adding small amounts of DES(A) to the solvent, which should not have any drawbacks as the DES would be present in the final composition anyways. After several tests, the solvent composition for the Heck reactants was set to DES(A):H_2O:EtOH = 1:2.25:6.75 (v:v:v). Together with the solvent of the enzymatic stock, the final solvent system in the Heck reactor is DES(A):KPi-buffer:H_2O:EtOH = 6:5:2.25:6.75 (v:v:v:v). This solvent was then also used in some of the batch experiments for further optimization experiments.

3.5 Basicity - Influence on Heck reactions

The type and amount of the applied base has a big impact on the performance of the Heck reaction. In this work, different concentrations of the following bases were tested:

- K_2CO_3
- Na_2CO_3
- NaOH

- NaOAc
- DIPEA
- Tributylamine

DIPEA and tributylamine were ruled out after preliminary experiments due to poor water solubility compared to the other bases. Moreover, it was decided against the amines in order to not introduce further organic compounds that could lead to side reactions.

The remaining bases (K_2CO_3, Na_2CO_3, NaOH and NaOAc) were tested in different concentrations under the same reaction conditions. **2a** (10.0 mol/l), **3a'** (11.0 mol/l, 1.10 mol eq.) and the appropriate amount of base (see Table 3) were dissolved in DES(A):KPi-buffer:H_2O:EtOH = 6:5:2.25:6.75 (v:v:v:v) (10 ml). Reference samples (100 µl) were taken after heating to 85 °C in an oil bath. Afterwards, palladium catalyst SCM-A (12.7 mg) were added and the timing started. Samples (100 µl) were taken after 5, 10, 20, 30 and 60 (70) min and analyzed by HPLC (method B, see section 4.12). Conversion of **2a** and yield of **4aa'** over time and the HPLC area ratio of **4aa':5aa'** at the end of the reaction were determined and compared.

Table 3. Overview of conducted experiments on the influence of the applied type and amount of base on Heck reactions. Amount given in mol eq. referring to limiting component **2a** or in volume in µl of a NaOH solution (1.0 mol/l)

Exp. #	Base	Amount	Exp. #	Base	Amount
#1	Na_2CO_3	4 eq.	#11	NaOH	12.5 µl
#2	Na_2CO_3	5 eq.	#12	NaOH	50 µl
#3	Na_2CO_3	5.77 eq.	#13	NaOH	100 µl
#4	Na_2CO_3	7eq.	#14	NaOH	200 µl
#5	Na_2CO_3	10 eq.	#15	NaOH	300 µl
#6	NaOAc	4 eq.	#16	K_2CO_3	3 eq.
#7	NaOAc	5 eq.	#17	K_2CO_3	4 eq.
#8	NaOAc	7 eq.	#18	K_2CO_3	5 eq.
#9	NaOAc	10 eq.	#19	K_2CO_3	5.77 eq.
#10	NaOAc	15 eq.			

The conversion of **2a** over time was an important parameter to investigate, especially regarding the first couple of minutes. As only limited reaction times are possible in continuous flow

experiments, it was more crucial to convert high amounts of substrate in a short period of time than to reach high conversions at the end of the batch experiments. K_2CO_3 and Na_2CO_3 showed the best performance, giving more than 55 % conversion after 10 min in most cases, also reaching over 80 % at the end of the run. In contrast, with NaOH and NaOAc not more than 30 % conversion were obtained after 10 min, except for #15 where almost 55 % were reached in the same period of time. The best performing experiments are shown separately once more in Figure 4 (A) for better comparability. Again, it can be seen that K_2CO_3 and Na_2CO_3 are the favorites with similar reaction progression. NaOH gave slightly lower conversions at high concentrations and the lowest conversions were observed using NaOAc as base.

Another important parameter is of course the yield of the main product **4aa'**. Figure 4 (B) shows the yield of **4aa'** for all experiments after 60 and 70 min, respectively. Like in the comparison of the conversions, K_2CO_3 (yellow) and Na_2CO_3 (blue) performed better than NaOH (brown) and NaOAc (green). The best result was achieved by #1 which was the only experiment with a yield higher than 20 %. Other experiments such as, #2 and #3 (Na_2CO_3), #16, #17 and #19 (K_2CO_3) and even #15 (NaOH) had good results with a yield of **4aa'** higher than 15 %. The lowest average yield was obtained with NaOAc with slightly over 5 %.

The last evaluated finding was the ratio between the desired product **4aa'** and the side product **5aa'**. For the calculation of the ratio, the area values given by the HPLC were used, because of the lack of a proper calibration for **5aa'**. The ratio is particularly interesting because of the difficulty of the separation of the two products. Concerning Na_2CO_3, a contrary trend in Figure 4 (C) is visible compared to the diagrams before. Whereas conversion and yield increase with lowering the base concentration, the product ratio shows the exact opposite. Experiment #1 which had the highest conversion and yield of all reaction gave only a ratio of just below 4. It was possible to increase the value and approach a ratio of 6 in #5, by raising the concentration of Na_2CO_3. The performance of K_2CO_3 was comparable to that of Na_2CO_3 and an average ratio little more than 4 was achieved. NaOH gave the poorest results with values lower than 3, besides one exception where a ratio over 6 was achieved (#14). Surprisingly, NaOAc gave the best ratios among all bases with values of at least 6 in #6. In experiment #7 almost a ratio of 10 was reached and in #10 no side product **5aa'** was found at all, which would result in an infinite ratio value.

All in all, Na_2CO_3 and K_2CO_3 turned out to be the most favorable bases for the Heck coupling with the best performance in conversion and yield. Even though, NaOAc gave a remarkable product ratio, the conversion of the substrates was too slow and the yield too low. The performance of NaOH was promising at certain concentrations but the carbonates prevail as superior bases for the given reaction. Despite Na_2CO_3 being slightly better in all considered categories, K_2CO_3 was chosen as base for the flow experiments due to the much higher water solubility. According to Sigma Aldrich safety data sheets the solubility of Na_2CO_3 is >217 g/l (20 °C)[61], whereas the solubility of K_2CO_3 is almost six times higher with 1120 g/l (20 °C)[62]. Since, it would be devastating if any sort of precipitation or phase separation occurs in the flow reactors, it was decided to go with K_2CO_3 as base instead of Na_2CO_3.

(A)

(B)

(C)
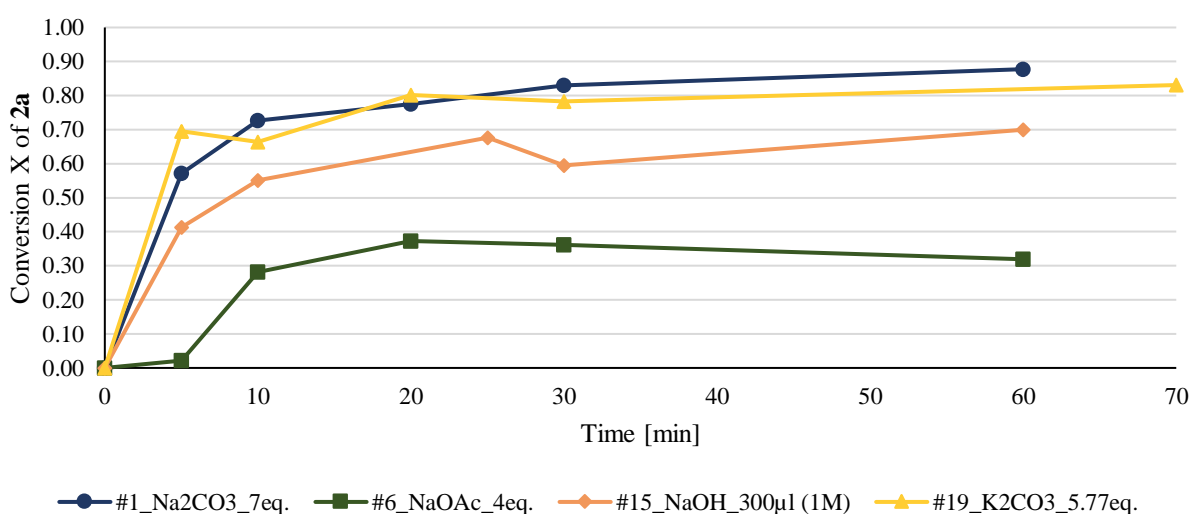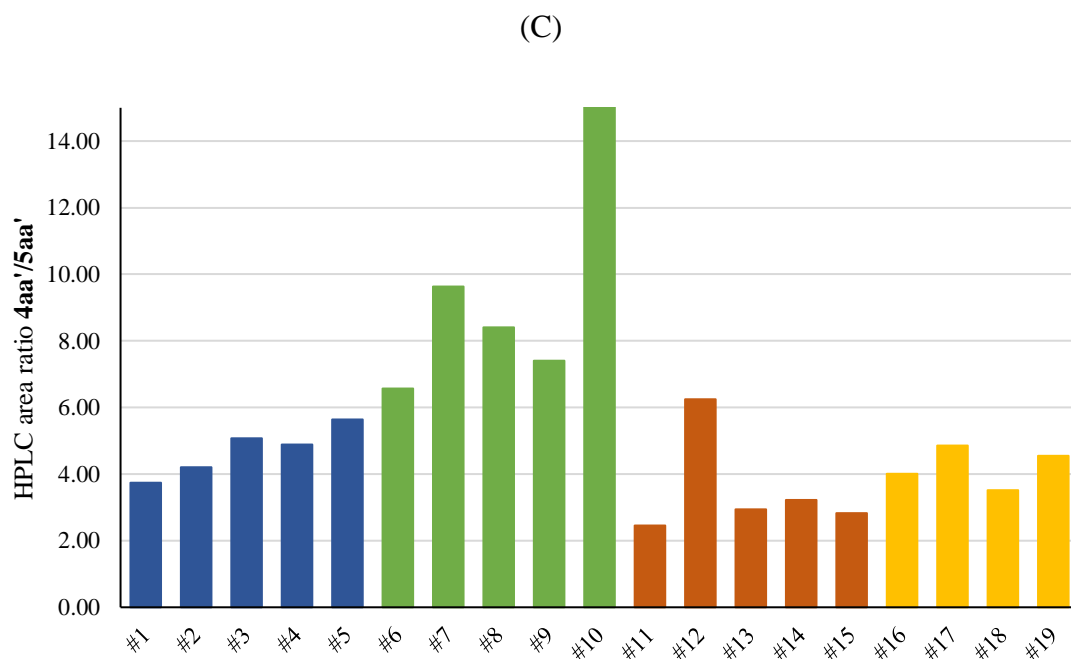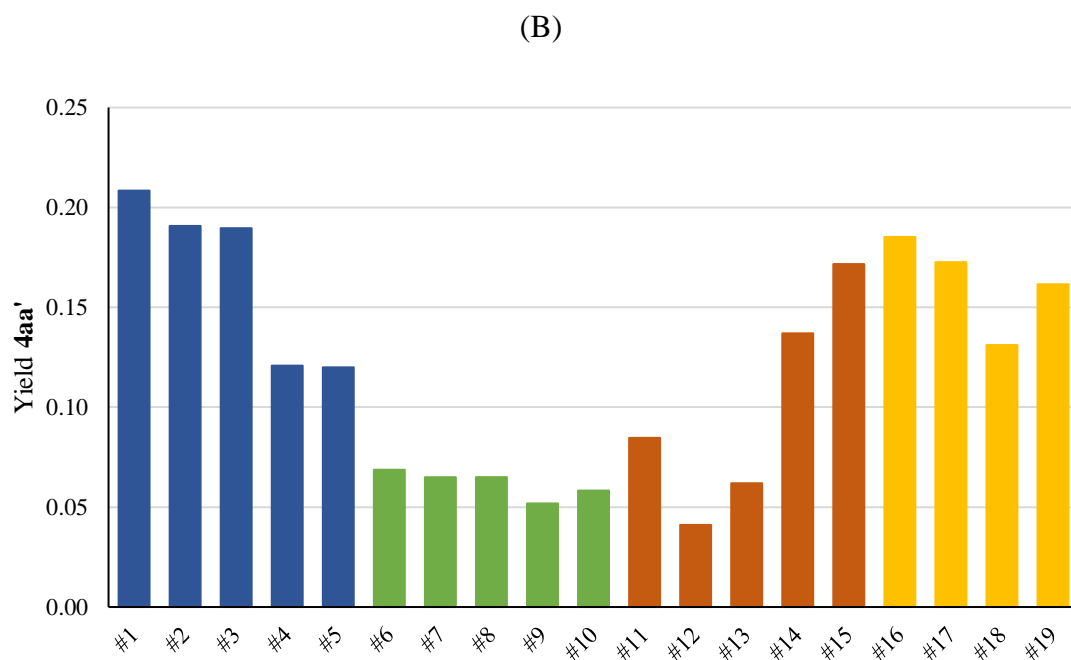
Figure 4. Influence of different bases and their concentration on the performance of Heck reactions. Data in "eq." are referring to mol equivalents of **2a** (10 mmol/l)

Coloration: blue: Na_2CO_3; green: NaOAc; brown: NaOH; yellow: K_2CO_3

(A) Best performing experiment of each base type concerning the conversion of **2a** over time.

(B) Yield of **4aa'** achieved with different bases and concentrations

(C) Ratio of the HPLC areas of **4aa'** relative to **5aa'** obtained with different bases and concentrations

3.6   Concentration of reactants – Influence on Heck reaction

The concentration of the reactants **2** and **3** was a further parameter to optimize for the Heck reaction. Several batch experiments were conducted with different concentrations and excess ratios. The effect of reagent concentrations on the reaction performance is shown in Figure 5. In this particular case, **2a** (10 mmol/l / 35 mmol/l) reacted with **3b'** (1.50 mol eq. referring. to **2a**) in the presence of K_2CO_3 (1.50 mol eq. ref. to **2a**). DES(A):KPi-buffer:H_2O:EtOH = 1:1:1:1 (v:v:v:v) (10 ml) served as solvent and SCM-A (12.7 mg) as catalyst. In both reactions, full conversion of **2a** was achieved, after 15 and 60 min, respectively. However, unlike the conversion, the yield of the product **4ab'** does not reach the same value at the end of the reactions, as it might be expected. In fact, only about half the yield can be achieved with 10 mmol/l compared to the experiment with 35 mmol/l.
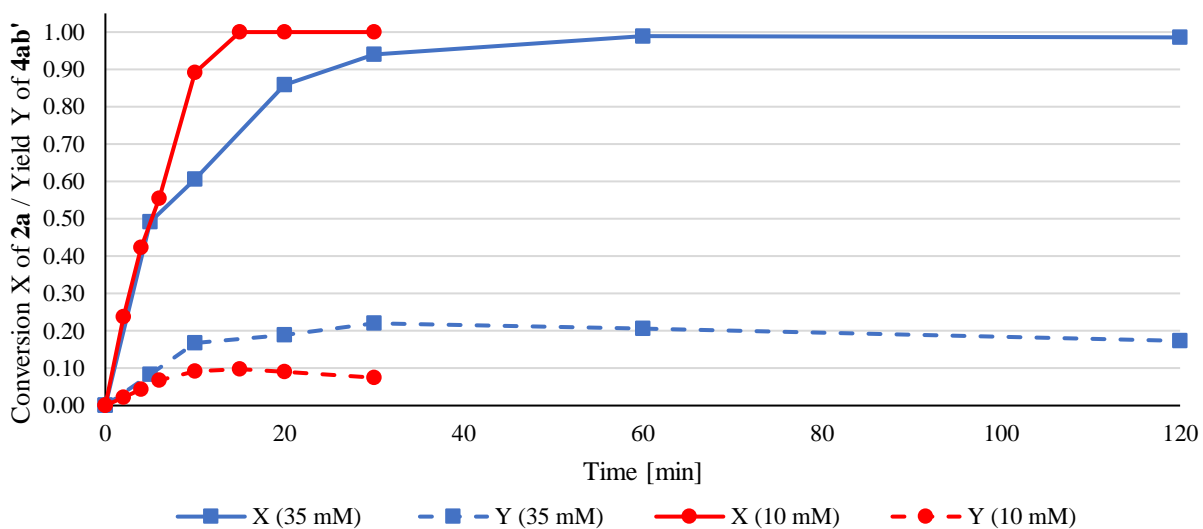
Figure 5. Conversion of **2a** and yield of **4ab'** over time of a Heck reaction with 35 mmol/l (blue) and 10 mmol/l (red) of the limiting **2a**. Reactant excess of **3b'** and base was 1.5 mol eq. referring to **2a**. Reaction temp.: 85 °C; Solvent: DES(A):KPi-buffer:H_2O:EtOH = 1:1:1:1 (v:v:v:v)

The primary reasons for this are the possible polymerization of **2a** and homo-coupling of **3b'**. Scheme 8 shows polymerization of the styrene derivative **2a** at the ethylene group and the catalytic homo-coupling of **3b'** by elimination of iodine. Even though these side reactions also occur at high concentrations, it seems that the effects become more relevant at lower concentration. Actually, this can be shown without comparing two experiments with different concentration. Looking at

the course of X and Y of the 35 mmol/l reaction in Figure 5, one can observe that the yield hardly changes after 10 min, although the conversion only reached 60 %. This means that most of the remaining 40 % of **2a** is consumed in the polymerization reaction and other possible side reaction.

4-vinylphenol   **polymer**   **4-iodophenol**   **[1,1'-biphenyl]-4,4'-diol**
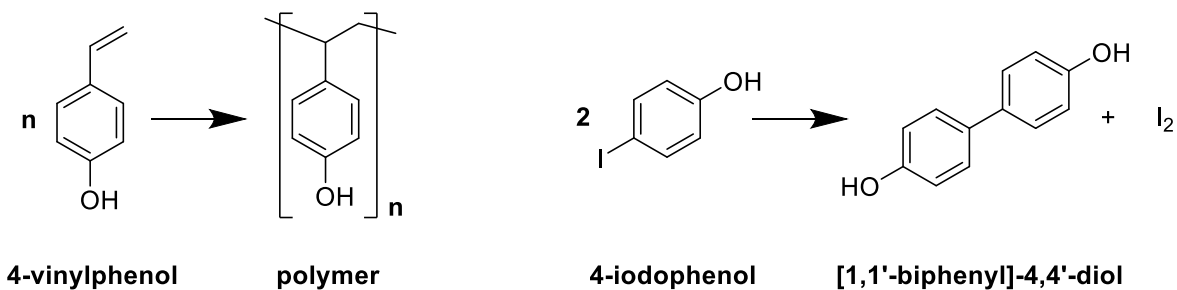
Scheme 8. Side reactions of **2a** (polymerization, left) and **3b'** (homo-coupling, right), same reactions apply for all other derivatives mentioned in this work

The conducted experiments led to the conclusion that high concentrations would favor the desired reaction. Unfortunately, there is a limitation for the continuous enzymatic decarboxylation reaction, which provides the substrates for the Heck coupling. The unsaturated acids **1a-e** used as starting materials are poorly soluble in the used solvent. For example, the water solubility of **1a** (*p*-coumaric acid) is 1.02 mg/ml[63] or 6.21 mmol/l. With DES(A):KPi-buffer = 1:1 as solvent the solubility was increased to slightly more than 20 mmol/l. However, considering the dilution in the mixing point of the flow reactor due to addition of a second stock containing the substrate for the subsequent Heck reaction, a maximum concentration of 10 mmol/l can be reached for the second step. Thus, low yields were expected in the combined flow reactions. One possibility to overcome the solubility problem is to feed a suspension of **1a** into to the reactor. More on that is shown in section 3.7. Another approach was to switch the molar ratio of educts **2a-2e** and **3a'-3b'**, in order to make the aryl iodide the limiting component because the vinyl components are reacting faster in side reactions than the aryl iodide. Moreover, it was decided to lower the reactant excess to 1.10 mol eq. referring to the limiting component in certain reactions (see sections 3.5, 3.7 and 3.9) to reduce undesired polymerization of **2a-2e**.

3.7 Continuous Heck reactions

After the optimization of the parameters in batch, continuous Heck reactions were performed to test the reaction conditions in a flow setup, before the final combined experiments.

First, two experiments (A1 and A2) with a packed column-S as reactor were performed. In these test runs, the influence of reagent concentration was investigated. As described before in section 3.6, the concentration of the intermediate **2a** will be at most 10 mol/l in the combined two-step setup due to solubility issues in the decarboxylation step. Nevertheless, the influence of the concentration should be shown for flow reactions as well. In Figure 6 the conversion (solid line) and the yield (dashed line) over time are compared (c(**2a**): 35.0 mmol/l (blue) and 10.0 mmol/l (red)). Like in the batch experiments the higher concentrated reactions performed slightly better, although the difference is not as significant as in batch. Experiment A1 (blue) averaged at about 85 % conversion of **2a** at a yield of 25 % of **4aa'** until 240 min reaction time. After that, the performance dropped to a conversion of 75 % and a yield of slightly above 20 %. This was most likely caused by an operational error during to the refilling of the syringe (20 ml) after 210 min. The effects of refilling are also observable at experiment A2 (red), with the difference that in this case the performance slightly improved. Around 90 % conversion and almost 20 % yield were reached at the end of the reaction.

The flow rates of both experiments slightly differ because two different pumps were used with different set-value calibrations (see section 4.1). This makes a comparison of the data difficult. Nevertheless, it can be assumed that the concentration does not have such a great influence in the flow experiments as it had in batch. Thus, lower concentration should not impact the outcome of the combined setup too much.
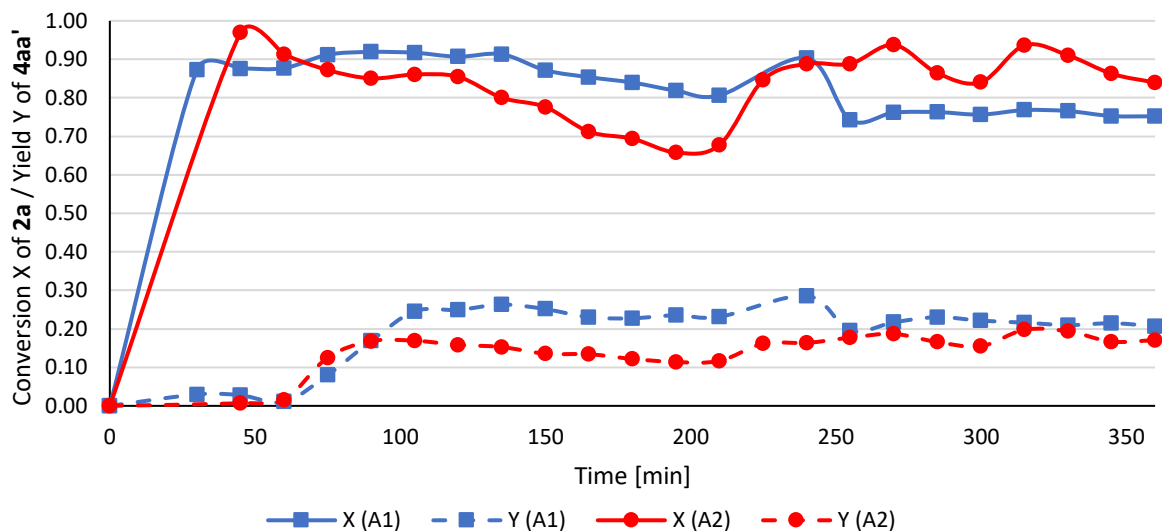
Figure 6. Influence of reactant concentration on continuous Heck reaction shown by comparison of conversion of **2a** (solid line) and yield of **4aa'** (dashed line) over time. Solvent: DES(A):KPi-buffer:H_2O:EtOH = 1:1:1:1 (v:v:v:v); Catalyst: SCM-A (1.8 g); 85 °C
A1 (blue): **2a** (35.0 mmol/l), **3a'** (52.5 mmol/l), K_2CO_3 (52.5 mmol/l), flow rate (0.102 ml/min)
A2 (red): **2a** (10.0 mmol/l), **3a'** (15.0 mmol/l), K_2CO_3 (52.5 mmol/l), flow rate (0.114 ml/min)

In the following two experiments (A3 and A4) the packed column-L served as flow reactor. This time the concentration of the Heck coupling reagent **3a'** was varied. In experiment A3 an excess of 1.50 mol eq. referring to **2a** was used, whereas in A4 **3a'** was the limiting component with a concentration of 9.1 mmol/l, so **2a** was in 1.10 mol eq. excess with a concentration of 10 mmol/l. Figure 7 shows the results of the experiments. In case of A3 (blue) the conversion (solid line) of **2a** and the yield (dashed line) of **4aa'** relative to **2a** is depicted. Analogous to that, in case of A4 (red) the conversion and the yield are calculated relative to the new limiting component **3a'**.

Experiment A3 gave full conversion over the whole course of the reaction, but interestingly, a yield can only be observed after 180 min. The yield then increased to about 20 % after reaching steady-state operation. In experiment A4, a conversion of **3a'** of about 85 % was achieved with an almost constant yield of little more than 10 % over the whole run. This means that a reactant ratio with **3a'** being the limiting component, is unfavorable for the outcome of the reaction, giving less conversion and only half the product yield the with **3a'** in excess.
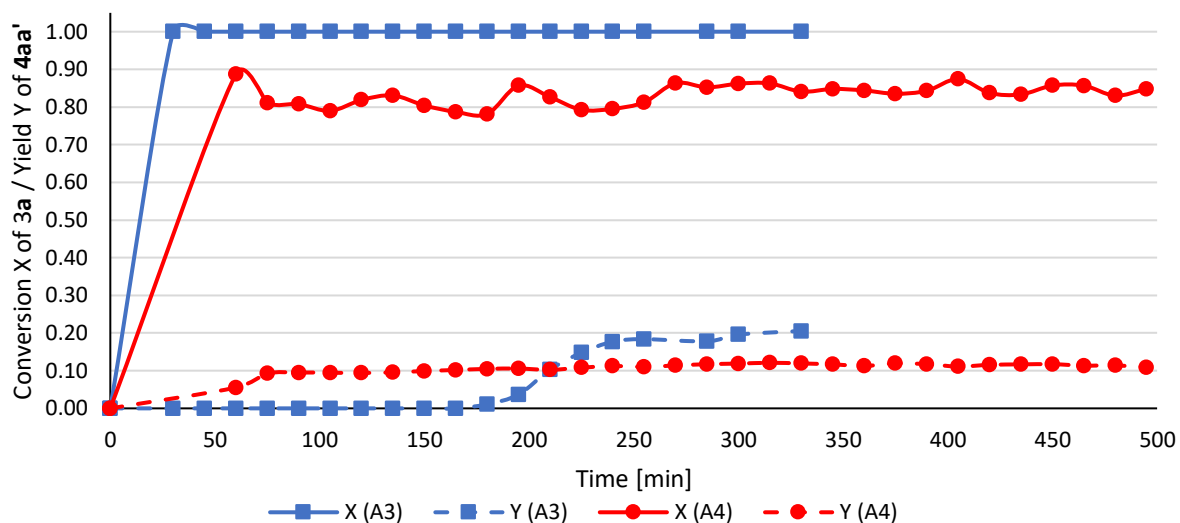
Figure 7. Influence of making **3a'** the limiting component and applying **2a** in excess on a continuous Heck reaction. Conversion of **2a** or **3a'** (solid line) and yield of **4aa'** (dashed line) related to limiting compound over time. Solvent: DES(A):KPi-buffer:H_2O:EtOH = 6:5:2.25:6.75 (v:v:v:v); Catalyst: SCM-A (5.5 g); 85 °C
A3 (blue): **2a** (10.0 mmol/l), **3a'** (15.0 mmol/l), K_2CO_3 (52.5 mmol/l), Flow rate (0.091 ml/min).
A4 (red): **2a** (10.0 mmol/l), **3a'** (9.1 mmol/l), K_2CO_3 (27.3 mmol/l), Flow rate (0.097 ml/min)

The last continuous Heck reaction (A5) was performed with **3b'** instead of **3a'** as coupling reagent. **2a** (10 mmol/l) was the limiting component and **3b'** was applied in excess (1.50 mol eq). With this setup a conversion of almost 98 % was achieved (see Figure 8), which is comparable to run A3. Unfortunately, there was no calibration for the product **4ab'**, thus no yield could be calculated. Nevertheless, the formation of the product can be tracked by the determined HPLC peak area in mAU·min (milli area units · minutes). Although no calibration for the product was available, it is shown that the yield approaches steady-state after about 240 min. As the two reactants **3a'** and **3b'** gave similar results in batch reactions, it can be assumed that the yield of this experiment would be between 10 and 20 %.
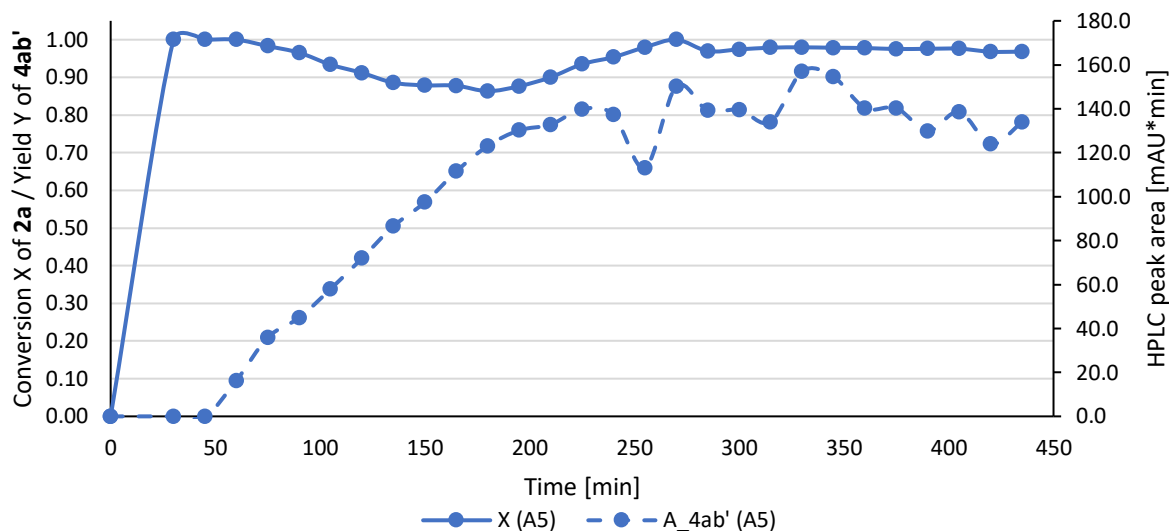
Figure 8 Conversion of **2a** and HPLC peak area of **4aa'** in mAU·min over time.
Solvent: DES(A):KPi-buffer:H$_2$O:EtOH = 6:5:2.25:6.75 (v:v:v:v); Catalyst: SCM-A (5.5 g) 85 °C
A5: **2a** (10.0 mmol/l), **3b'** (9.1 mmol/l), K$_2$CO$_3$ (27.3 mmol/l), Flow rate: 0.097 ml/min

3.8   Combined flow experiments

The combined flow setup was a fully integrated reaction cascade including an enzymatic decarboxylation with immobilized *Bs*PAD beads and a palladium-catalyzed Heck reaction with the heterogeneous catalyst SCM-A (Ce$_{0.20}$Sn$_{0.79}$Pd$_{0.01}$O$_{2-\delta}$). In Scheme 9, a general flow scheme of the two-step setup is shown. In all of the combined setups, only **1a** and **3a'** were used as reactants, thus only **2a** and **4aa'** (**5aa'**) were synthesized as intermediate and products, respectively. As the applicability of other derivatives was already confirmed in single-step reactions, combined experiments were left out due to time limitations. The decarboxylation and Heck reaction were conducted at 30 and 85 °C, respectively.
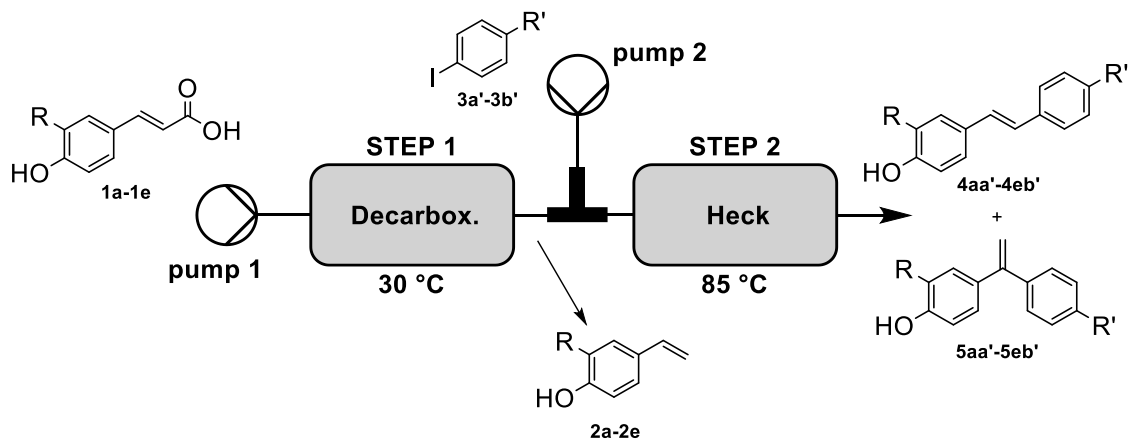
Scheme 9. General flow chart of the combined two-step reaction setup with an enzymatic decarboxylation followed by a palladium-catalyzed Heck reaction

a: R = H   a': R = H
b: R = OMe   b': R = OH
c: R = F
d: R = Cl
e: R = Br

The two-step reaction was performed in three different setup variations. For the first experiment (B1), column-L (HPLC column: L x I.D. = 120 x 8 mm) for the decarboxylation and column-S (HPLC column: L x I.D. = 40 x 8 mm) for the Heck reaction was chosen. The results of the run are shown in Figure 9. A conversion of **1a** of around 99 % was achieved over the whole reaction. This confirms that the amount of enzyme (160 mg immobilized in 2 % (w/v) alginate (4 ml)) was sufficient for a concentration of 20 mmol/l of substrate, thus the decarboxylation step worked properly. In contrast to that, the Heck reaction seems incomplete, as there is a high concentration of **2a** found in the outflow. Interestingly, despite the seemingly low conversion of the intermediate, the yield of the desired product **4aa'** was well above 25 % in the last few samples.
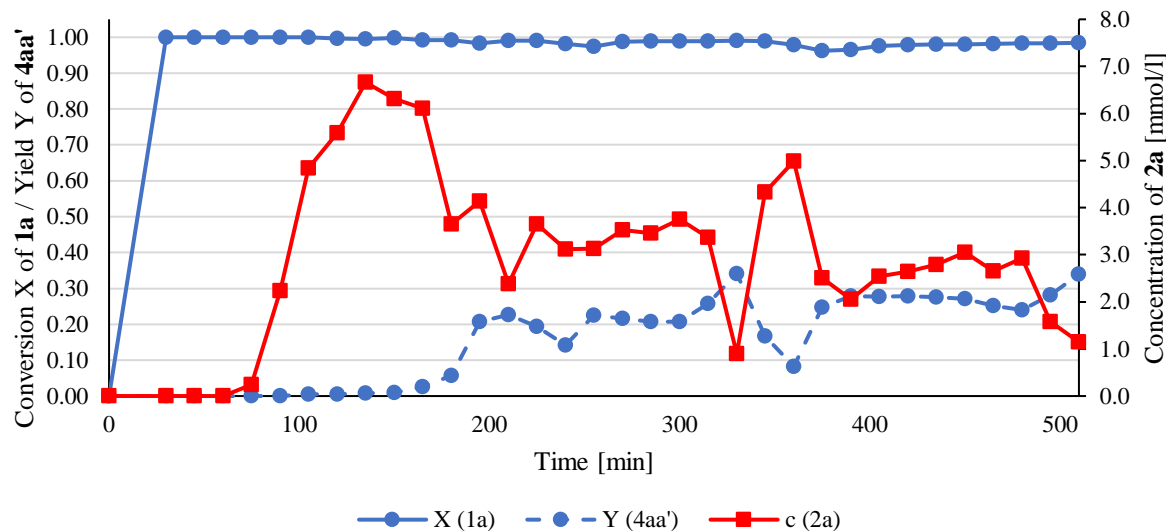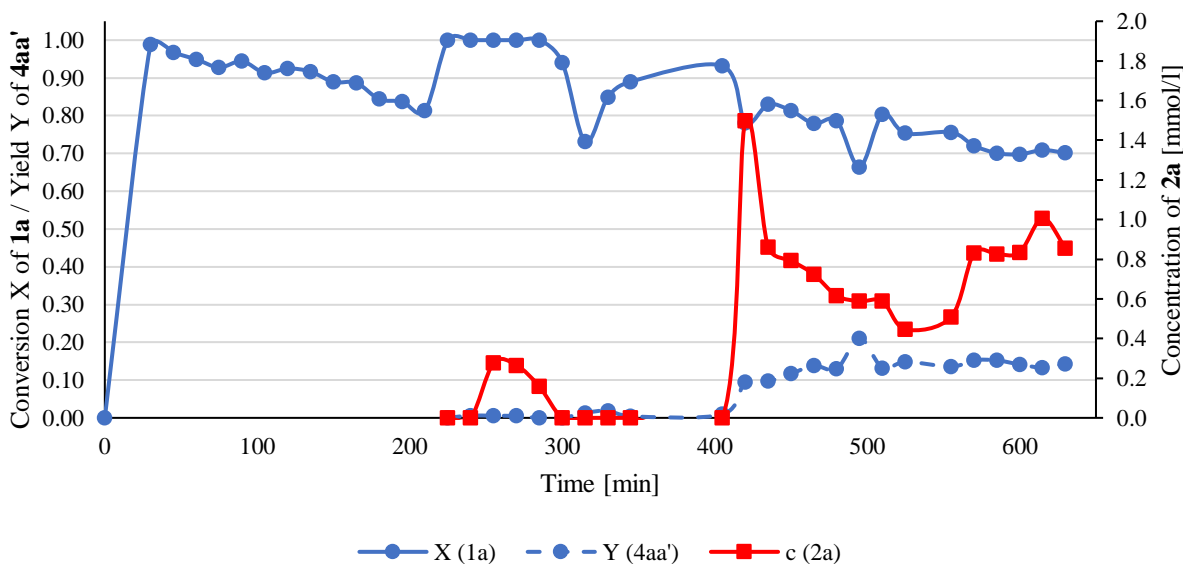
Figure 9. Conversion of **1a** (blue, solid line), yield of **4aa'** (blue, dashed line) and concentration c of **2a** (red) over time in a two-step continuous reaction with decarboxylation in column-L (30 °C) and Heck coupling in column-S (85 °C). Starting concentration of **2a**: 20 mmol/l; 1.50 molar excess of **3a'** (30.0 mmol/l); K_2CO_3 105.0 mmol/l; flow rate pump 1: 0.097 ml/min; flow rate pump 2: 0.091 mmol/l; 160 mg *Bs*PAD; 1.8 g SCM-A

To improve the findings of B1, in experiment B2 the reactor configuration was changed. Two column-Ss were used for the decarboxylation step and column-L for the Heck reaction. This should enhance the performance of the Heck coupling, as the catalyst amount and the residence time in the reactor were three times higher than in the previous run. The amount of enzyme was kept constant. As given in Figure 10, the conversion of **1a** was around 99 % as expected. Unfortunately, even though the intermediate **2a** was fully converted during steady-state operation (spikes in concentration caused by syringe refilling), the yield of the product only averaged a value of 21 %, which is even less than the yield in experiment B1 where much less of catalyst was used. This leads to the conclusion that the Heck coupling happens very quickly and most of the product is formed in the first part of the reactor. However, the location of the thermodynamic reaction equilibrium of this reaction most likely does not allow a higher product concentration. This could explain why the yield hardly ever exceeds more than 25 % neither in batch nor in continuous flow reactions. As shown, longer residence times in the reactor only causes conversion of the intermediate into different kinds of side products (see also polymerization and homo-coupling in section 3.6). Furthermore, side reactions of the formed product **4aa'** might occur, which explains a slightly lower yield in experiment B2 compared to B1.

Disregarding the low yield, it was possible to develop a consistently operating process. As demonstrated in experiment B2, it is possible to perform the targeted two-step reaction, including an enzymatic decarboxylation and a palladium-catalyzed Heck reaction for almost 24 h in steady-state without major operational difficulties.
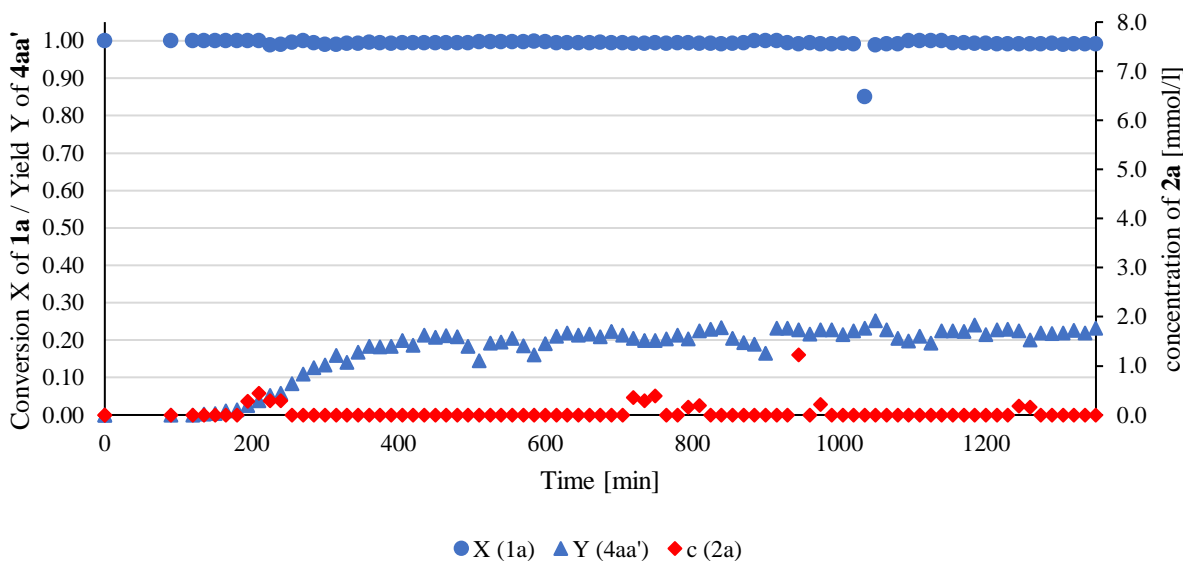
Figure 10. Conversion of **1a** (blue dots), yield of **4aa'** (blue triangles) and concentration c of **2a** (red) over time in a two-step continuous reaction with decarboxylation in 2x column-S (30 °C) and Heck coupling in column-L (85 °C). Starting concentration of **2a**: 20 mmol/l; 1.50 molar excess of **3a'** (30.0 mmol/l); K$_2$CO$_3$ 105.0 mmol/l; flow rate pump 1: 0.097 mmol/l; flow rate pump 2: 0.091 mmol/l; 160 mg *Bs*PAD; 5.5 g SCM-A

The last approach of combined continuous flow reactions (B3) was performed using a 3D-printed continuous stirred tank reactor (CSTR) for the enzymatic decarboxylation and column-L for the Heck coupling. This time the amount of **1a** was increased by using a suspension with a loading of 45.0 mmol/l. In order to ensure a constant composition of the substrate feed, the suspension was stirred in a beaker to obtain an even distribution of the substrate particles and a peristaltic pump fed the stock into the CSTR. Figure 11 shows the results achieved by using this setup. At the beginning of the experiment, the decarboxylation was tested individually to get an insight on the performance of the CSTR. The conversion of **1a** slightly decreases over time but nevertheless more than 90 % were observed for almost 3 hours. Most importantly, the solid particles of the suspension dissolved in the reactor as the reaction as the reaction proceeded processed and a clear solution was obtained at the outflow. It is crucial to have a homogeneous solution without particles for the subsequent reaction step to avoid clogging of the filters of the packed bed reactor. After 225 min

the whole setup was assembled and the combined experiment started. The spikes in the diagram are caused by short stoppage of the material flow in order to refill the syringe with Heck reactant stock (**3a** and K_2CO_3). After about 550 min overall reaction time steady-state was reached. The conversion of **1a** was around 70 % and a yield of **4aa'** of about 15 % was observed. Further, the intermediate **2a** was not fully converted like in run B2, with a residual amount of nearly 1 mmol/l. Compared to experiment B1 and B2, this setup gives the lowest yield of the desired product relative to the substrate. However, the concentration of the substrate is much higher in this setup, thus the absolute amount of the product in B3 is higher than in the other experiments. The concentration of **4aa'** at the end of the runs averaged 3.2 mmol/l in B3 and 2.3 mmol/l in B2.

It was shown that increasing the substrate concentration does not enhance the formation of the desired product as expected. Raising the concentration from 20 to 45 mmol/l (factor of 2.25) only changes the product concentration from 2.3 to 3.2 mmol/l (factor of 1.4). This again leads to the conclusion that the formation of **4aa'** is simply limited by the reaction equilibrium. Thus, even higher substrate concentrations with more enzyme and palladium catalyst would not necessarily improve the outcome of the reaction sequence.

Figure 11. Conversion of **1a** (blue, solid line), yield of **4aa'** (blue, dashed line) and concentration c of **2a** (red) over time in a two-step continuous reaction with decarboxylation in CSTR (30 °C) and Heck coupling in column-L (85 °C). At the beginning only decarboxylation reaction and after 225 min two-step reaction. Starting concentration of **2a**: 20 mmol/l; 1.50 molar excess of **3a'** (49.5 mmol/l); K_2CO_3 81.9 mmol/l; flow rate pump 1: 0.097 mmol/l; flow rate pump 2: 0.091 mmol/l; 160 mg *Bs*PAD; 5.5 g SCM-A

3.9 Further substrates

As the feasibility of the setup was proven, also other substrates should be tested. The reactions of the substituted derivatives of *p*-coumaric acid **1b-1e** (see also Table 4) are mentioned separately because of limited access to the substrates and the very specific experiments, which were only conducted once. The substrates were obtained as pure powder from the Institute of Molecular Biotechnology, TU Graz.

The procedure for the substituted acids starts with a continuous decarboxylation and is followed by a Heck reaction in batch after isolation of the intermediates. Figure 12 shows the conversions of the substrates over time for the enzymatic decarboxylation. All experiments gave high conversions at a flow rate of 0.091 ml/min. The F-substituted substrate **1c** had the highest conversion with >99 % over the whole course of the experiment. Also, for all other substrates a conversion of at least 94 % was observed. The average conversion and yield are summarized in Table 4. These tests confirmed the applicability of substituted *p*-coumaric acid derivatives in continuous decarboxylation.
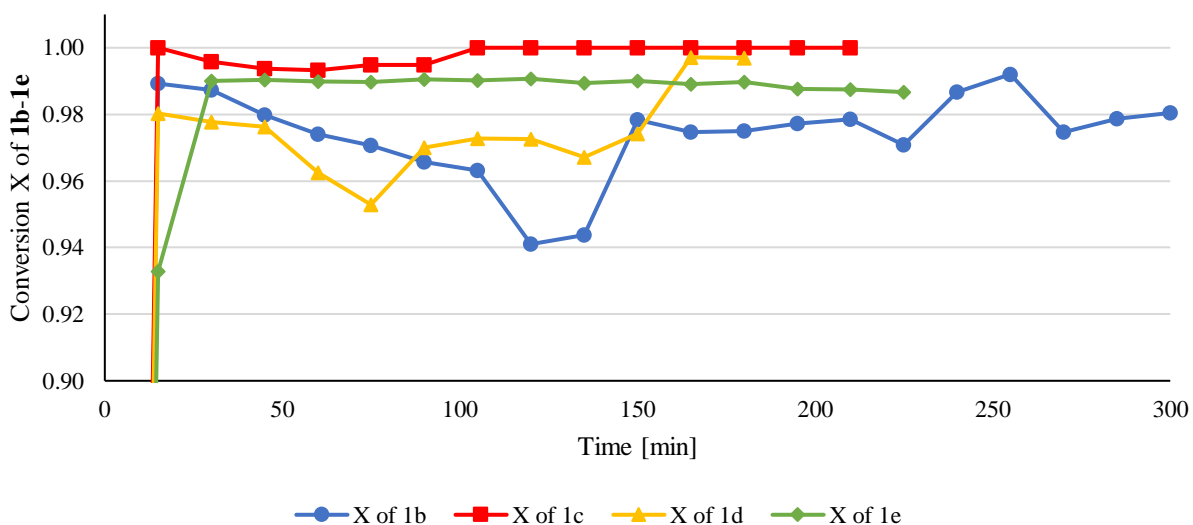
Figure 12. Conversion of substituted *p*-coummaric acids **1b-1e** (**b**: 3-methoxy; **c**: 3-fluoro; **d**: 3-chloro; **e**: 3-bromo) over time during the continuous decarboxylation with immobilized *Bs*PAD (160 mg in 2 % (w/v) alginate (4 ml)). 20 mmol/l substrate in DES(A):KPi-buffer = 1:1 (v:v) at 30 °C. Flow rate 0.091 ml/min.

After the decarboxylation, all the isolated intermediate was used for the Heck reaction in batch. In Figure 13 the conversions of **2b-2e** over time are given. Like in the continuous decarboxylation

experiments, the F-substituted compound **2c** showed the best results with a conversion of almost 98 % after 120 min and 99 % at the end of the run (240 min). Also, the Cl-intermediate **2d** had a high reactivity, reaching 93 % conversion. The Br- and MeO-compounds **2e** and **2b** showed similar results with **2b** reacting a bit slower. Both reactions reached a conversion of around 85 %. As shown, the halogen-substituted intermediates have a higher reactivity in the Heck reaction than the MeO-derivative but all substances gave good results in the batch experiments and would most likely be usable for continuous Heck reactions as well.
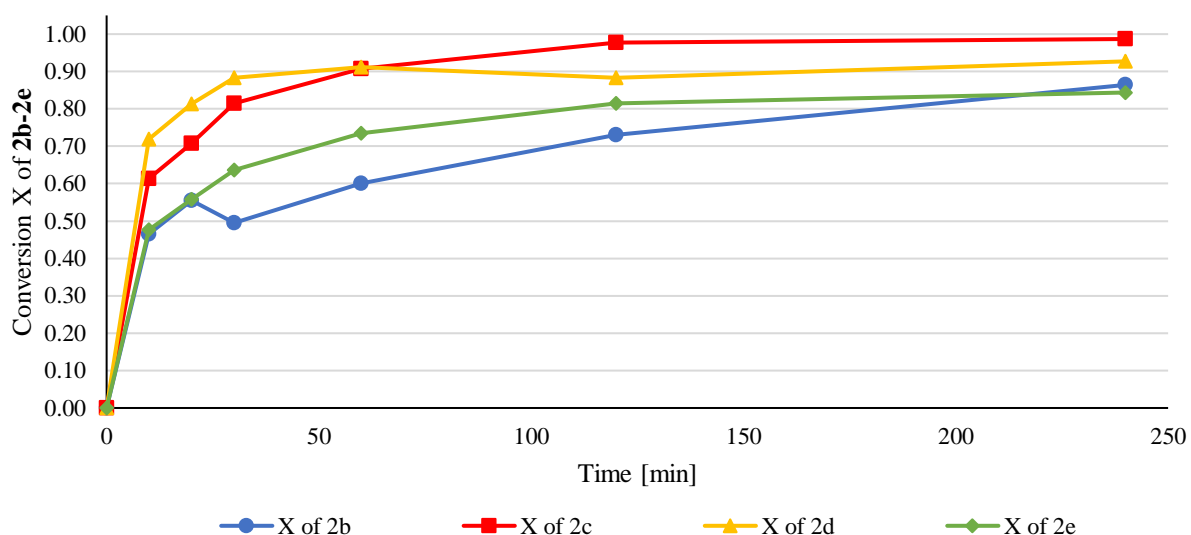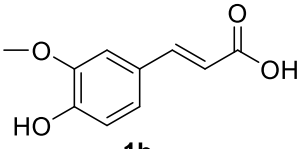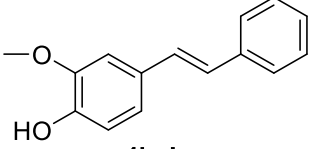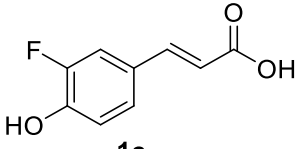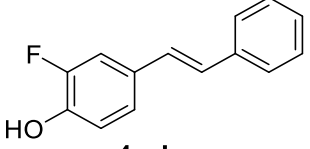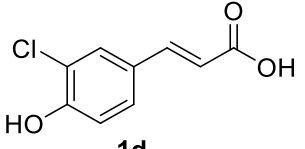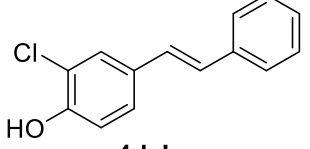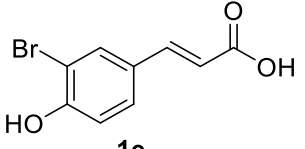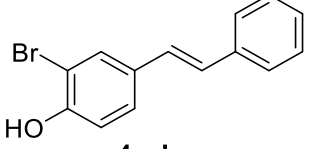
Figure 13. Conversion of substituted 4-vinylphenols 2**b-2e** (**b**: 3-methoxy; **c**: 3-fluoro; **d**: 3-chloro; **e**: 3-bromo) over time in a batch Heck reaction at 85 °C. Solvent: DES(A):KPi-buffer:H$_2$O:EtOH = 6:5:2.25:6.75 (v:v:v:v); Starting concentration: 10 mmol/l; . Reactant excess of **3a'** and base was 1.5 mol eq. referring to **2a** Catalyst: 12.7 mg SCM-A

It was possible to show the applicability of different *p*-coumaric acid derivatives in the developed two-step reaction cascade. Both continuous decarboxylation and Heck coupling gave good results in terms of conversion and reaction rate. The observed results are summarized in Table 4. Unfortunately, due to limited access of the substrates neither a calibration of substrates and products nor a combined continuous experiment was possible. Nevertheless, it was shown that the continuous decarboxylation is fast enough to provide fair amounts of intermediate for a subsequent reaction step. Moreover, the Heck reactions in batch delivered satisfying results, hence it can be

assumed that a combined continuous setup is suitable for the substituted derivatives of *p*-coumaric acid.

Table 4. Summary of results of continuous decarboxylation of **1b-1e** and batch Heck reaction of **2b-2e**. For the decarboxylation the average conversion X (after reaching steady-state operation) of the substrate and the isolated yield of the intermediate **2b-2e** are shown. For the Heck reaction the conversion X of the intermediate at the end of the run (240 min) and the isolated yield Y of the product **4ba'-ea'.** *isolated yield was not further purified after extraction. Thus, the given masses of the intermediates and products should be considered as crude yield.

Substrate	Enzy. decarbox.		Heck reaction		Product
	aver. X	iso. Y*	X	iso. Y*	
1b	97 %	23.3 mg	86 %	35.9 mg	**4ba'**
1c	>99 %	32.8 mg	99 %	39.5 mg	**4ca'**
1d	98 %	53.2 mg	93 %	23.9 mg	**4da'**
1e	99 %	36.8 mg	84 %	41.6 mg	**4ea'**

3.10 Rearrangement reaction of 5aa' to 4aa'

During Heck reactions in batch, a shift in the ratio of the product **4aa'** to the side product **5aa'** (in favor of the desired product) was observed over time. Therefore, several experiments were conducted to investigate a possible rearrangement reaction of **5aa'** to **4aa'** in presence of palladium catalyst and elevated temperatures, as shown in Scheme 10. (NMR-spectra of **4aa'** and **5aa'** are shown in the appendix section 6.2)
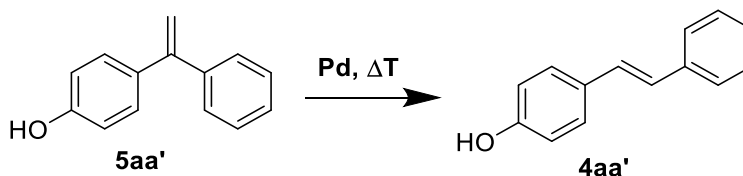
Scheme 10. Proposed rearrangement reaction of **5aa'** to **4aa'**

Out of the five experiments described in section 4.11 the two best working reactions (C3 and C4) are shown to illustrate the progress of the rearrangement reaction over time. As there was no proper calibration of the side product, other ways of quantification have to be found to assess the reaction outcome. To do so, the ratio (AR_t) of the peak areas ($A_{4aa'}$ and $A_{5aa'}$) determined by HPLC measurements and the relative gain of this ratio in percent ($\%gain_t$) were calculated as follows:

$$AR_t = \frac{A_{4aa',t}}{A_{5aa',t}} \tag{1}$$

$$\%gain_t = \frac{AR_t - AR_{t=0}}{AR_{t=0}} \cdot 100\ \% \tag{2}$$

The index t represents a certain reaction time. These values allow to track the progress of the rearrangement reaction without calibration. In Figure 14 the AR_t (solid line) and the $\%gain_t$ (dashed line) of experiment C3 (blue) and C4 (red) (see section 4.11) are shown. In both cases an increase of the graphs over time can be observed, which means there was formation of the desired product **4aa'** while the concentration of **5aa'** decreased. Despite the reaction being very slow by only reaching around a 10 % higher ratio after 240 min and at most 16 % after 360 min, it was possible to show that there is the possibility to perform a catalytic rearrangement reaction at elevated temperatures to enhance the product yield.

Due to time limitations, no further investigations on this reaction were performed but it was observed that the initial concentration and amount of catalyst and base have an influence on the outcome of the rearrangement. Most likely, a variation of the reaction temperature would have a big impact too (see temperature dependency in section 3.2) and also the solvent composition should be considered as a parameter for further improvements.

To my knowledge no similar rearrangement reaction of 4-(1-phenylvinyl)phenol (**5aa'**) to 4-hydroxystilbene (**4aa'**) with palladium as catalyst is reported in literature.
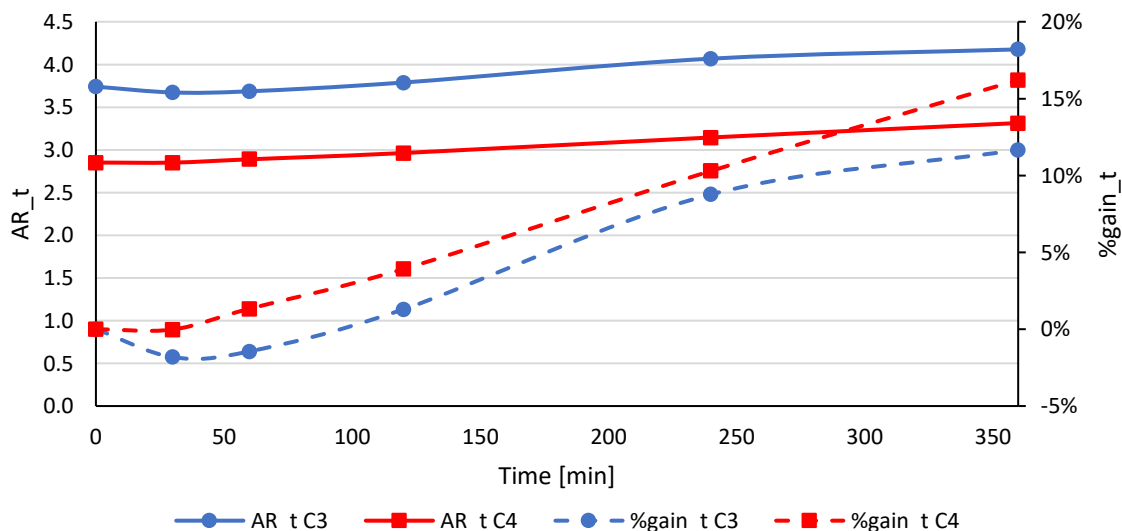
Figure 14. Illustration of the catalytic rearrangement of **5aa'** to **4aa'** at 85 °C. AR_t of **4aa'** to **5aa'** is shown to visualize the increase in **4aa'** and the decrease of **5aa'** (solid lines). The %gain represents the gain of area ratio in percent over time referring to the initial area ratio of the products (dashed lines). Solvent: DES(A):KPi-buffer:H_2O:EtOH = 6:5:2.25:6.75 (v:v:v:v) (5 ml).
C3: product mixture (25 mg); K_2CO_3 (37.73 mg); SCM-A (25 mg)
C4: product mixture (10 mg); K_2CO_3 (18.8 mg); SCM-A (10 mg)

4 Experimental

The two-step syntheses of the resveratrol derivatives **4aa'-4eb'** were performed combining an enzymatic decarboxylation and a subsequent palladium-catalyzed Heck coupling. Different experimental setups and reactor types were tried. The optimization of the process conditions was mainly determined in batch. All procedures and equipment are described in more detail in the following sections.

The enzyme *Bs*PAD and the substituted *p*-coumaric acid derivatives **1b**-**1e** were obtained from the Institute of Molecular Biotechnology, TU Graz. All other chemicals and solvents were purchased from Sigma Aldrich and utilized as obtained from the supplier.

4.1 Equipment

4.1.1 Packed bed reactors

Preparative HPLC columns served as packed bed reactors for the continuous flow decarboxylation and Heck reactions. The columns were filled with enzyme beads or palladium-catalyst powder. Two different column models were used (see Figure 15), which will be abbreviated as column-L (long) and column-S (short) throughout the thesis. Column dimensions:

- column-L: L x I.D. = 120 x 8 mm
- column-S: L x I.D. = 40 x 8 mm

Figure 15. HPLC column-L: L x I.D. 120 x 8 mm (top); HPLC column-S: L x I.D. 40 x 8 mm (bottom left); filter, sealing ring, sealing cap, column cap (bottom right)

4.1.2   3D-printed continuous stirred tank reactor (CSTR)

A 3D-printed continuous stirred tank reactor (CSTR) filled with alginate beads containing immobilized *Bs*PAD was used for the enzymatic decarboxylation. The reactor consisted of two parts as shown in Figure 16. The top part (lid) was designed with an integrated sieve, which held back the beads and ensures a steady outflow of the fluid phase through the primary material outlet. An ordinary rubber ring that was put in the intended gap served as sealing. The reactor body consisted of a heating/cooling jacket with an in- and outlet, a material inlet and the secondary material outlet, which was not used as the reaction solution flowed through the lid of the CSTR. Thus, the secondary outlet was sealed with an HPLC fitting. The reactor was assembled and fixed finger tight with screws and nuts.

CSTR dimensions:

- Reaction zone: I.H. x I.D. = 26 x 20 mm
- Reactor Height (without lid): H = 34 mm
- Heating/cooling jacked: I.D. = 31 mm
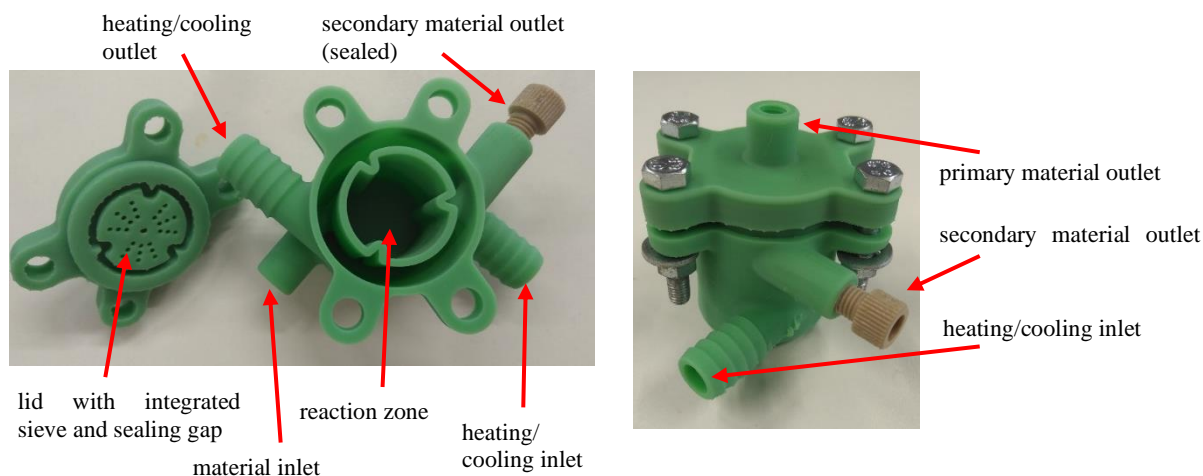
Figure 16. 3D-printed CSTR used for the continuous decarboxylation reactions; left: open CSTR with view on integrated sieve and sealing gap of the CSTR lid and the reaction zone in the CSTR body; right: assembled CSTR as it was used

The used 3D-printer was a "Anycubic Photon" based on an LCD (liquid crystal display) SLA (stereolithography apparatus) printing technology (see Figure 17). It is equipped with a UV light-source (wavelength = 405 nm), which provides an xy-DPI (dots per inch) of 47 µm (2560 x 1440),

a y-axis resolution of 1.25 µm and a layer resolution of 25 – 100 µm. With a printing speed of 20 mm/h and the maximum printing volume is 115 x 65 x 155 mm (length x width x height).

For the CSTR a green "Technology Outlet" 3D-print resin was used (see Figure 17).

Figure 17. left: Anycubic Photon 3D-printer; right: Technology Outlet 3D print resin (green)

4.1.3   Pumps

- HPLC pumps: P4.1S (Knauer; AZURA® Compact; max. flow rate: 5 ml/min)
- Syringe pumps**:** LA-120 (Landgraf Laborsysteme HLL; 2-channel; max. syringe volume: 60 ml), used syringe: 20 ml stainless-steel syringe. Pump rate is set indirectly by set-values that correspond to certain flow rates (calibration needed).
- Peristaltic pump: ISMATEC REGLO Digital MS-4/8 ISM 834C

4.1.4   Capillaries and fittings

The used capillaries, fittings and syringe adapters were standard HPLC equipment.

Inner diameter capillaries: 0.03 inch (0.762 mm)

4.1.5 Back pressure regulator (BPR)

P-762, BPR Cartridge 75 psi (5.17 bar) Gold Coat (IDEX Health & Science)

4.1.6 Thin layer chromatography (TLC) plates

TLC Silica gel 60 F_{254}, Aluminium sheets 20 x 20 cm from Merck

4.2 Preparation of the Deep Eutectic Solvent (DES)

To form a deep eutectic solvent (DES), a quaternary ammonium salt (QAS) and a hydrogen bond donor (HBD) was applied. In this work choline chloride (ChCl) served as salt and either glycerol, 1,2-propane diol, ethylene glycol or phenol were used as HBD (see Table 5). The ratio of the components was ChCl:HBD = 1:2 (mol/mol). The two staring materials were weighted in a beaker or Erlenmeyer flask and stirred for one hour at 85 °C in an oil bath. During this process, the choline chloride dissolved and a clear viscous liquid emerged, which stays clear even after cooling down to room temperature.

Table 5. Overview of used DES with the respective HBD and the molar ratio of ChCl to HBD

DES	QAS	HBD	ratio (mol:mol)
A		glycerol	
B		1,2-propane diol	
	ChCl		1:2
C		ethylene glycol	
D		phenol	

4.3 Preparation of potassium phosphate buffer (KPi-buffer)

The used buffer (KPi-buffer) was prepared by dissolving KH_2PO_4 (2.99 g, 21.97 mmol) and K_2HPO_4 (0.53 g, 3.04 mmol) in purified water (500 ml). This gave the required pH-value of 6 for an optimal enzyme performance during the decarboxylation reactions.

4.4 Enzyme immobilization – alginate beads

For the application of *Bs*PAD in heterogeneous reactions, the encapsulation in alginate beads was chosen as method to immobilize the enzyme. CFE (80.0 mg, Cell-free extract freeze-dried powder

containing *Bs*PAD obtained from the Institute of Molecular Biotechnology, TU Graz) and sodium alginate (40 mg) were dissolved in KPi-buffer (2 ml) and a yellowish viscous solution was obtained. The liquid was added dropwise to a 2 % (w/v) $BaCl_2$-solution under gentle stirring using syringe and needle (I.D. = 0.8 mm). It should be noted that the beads were dropped from a height of about 20 cm to obtain smooth spheres instead of droplet-shaped beads. As the beads enter the $BaCl_2$ solution they start to solidify. After 1 hour of gentle stirring, the beads were filtered and washed with 0.9 % (w/v) NaCl-solution. Then, the beads were dried on paper towels for 30 min under ambient conditions to improve their surface resistance. Afterwards, the immobilized enzyme beads (D = 2 mm) can be used as such.

4.5   Catalyst synthesis

4.5.1   Knitting aryl network polymers palladium catalyst (KAP-Pd)

For the immobilization of palladium on an organic support a slightly modified method of the reported Knitting Aryl Network Polymers (KAP) by Li *et. al.*[64] was used.

A solution of benzene (1.56 g, 0.02 mol), triphenylphosphine (5.25 g, 0.02 mol) and formaldehyde dimethyl acetal (4.56 g, 0.06 mol) in 1,2-dicholoroethane (20 ml) was prepared in a 100 ml round bottom flask. Then, iron(III) chloride (anhydrous, 9.75 g, 0.06 mol) was added to the solution. The emerging reaction was highly exothermic at the beginning, consequently the solution was stirred immediately in a cold-water bath. After 5 min the mixture was put into an oil bath where it was stirred for another 5 h at room temperature to form the crude aryl network. During the reaction the black mixture partly solidifies due to the polymerization reaction, which stalled the stir bar eventually. Afterwards, the oil bath was heated to 80 °C, where the reaction was finalized under reflux for another 67 h. Then, the KAP was washed with methanol (3 x 20 ml) and later extracted with methanol in a Soxhlet (70 ml, thimble: I.D. x H = 28 x 80 mm) apparatus for 24 h. Finally, the KAP was dried in a rotary evaporator under reduced pressure at 60 °C for 24 h and a fine brown polymer powder was obtained. For the immobilization of the palladium on the aryl network, KAP (2.0 g) was dispersed in acetonitrile (50 ml). Then, palladium(II) chloride (0.2 g, 0.56 mmol) was added to the suspension and stirred at 80 °C for 16 h. The product was filtered and washed with acetone (2 x 20 ml) and extracted with acetone in a Soxhlet (70 ml, thimble: I.D. x H = 28 x

80 mm) for 24 h. After drying in a rotary evaporator under reduced pressure at 60 °C for 24 h, the final KAP-Pd catalyst was obtained.

4.5.2   Solution combustion method (SCM)

The solution combustion method (SCM) first reported by Baidya *et. al.*[65] and modified by Lichtenegger *et. al.*[66] was used to prepare a highly porous Ce-Sn-Pd-oxide. The catalysts with the formula $Ce_{0.99-x}Sn_xPd_{0.01}O_{2-\delta}$ (x = 0.79, 0.99) consists of a cerium and tin oxide support with palladium as catalytically active species.

For the synthesis of the catalyst the appropriate amounts (see Table 6) of ammonium cerium(IV) nitrate $((NH_4)_2Ce(NO_3)_6)$, tin(II) oxalate (SnC_2O_4), glycine $(C_2H_5NO_2)$ and palladium(II) chloride $(PdCl_2)$ were pestled in a mortar until a fine and homogeneous powder was obtained. Afterwards, water (6 ml) was added to the mixture and filled into a 600 ml beaker and homogenized in an ultra-sonic bath for 30 min, giving a dark-brown viscous suspension. Then, the mixture was heated to 350 °C for 1 h for the combustion reaction in a muffle furnace. The obtained voluminous preliminary catalyst was again pestled in a mortar. Finally, the catalyst was heated to 350 °C over night for the calcination of the powder and the obtained final catalyst was used as such for the reactions.

Table 6. Required amounts of starting materials for the synthesis of 9 g of $Ce_{0.99-x}Sn_xPd_{0.01}O_{2-\delta}$

$Ce_{0.99-x}Sn_xPd_{0.01}O_{2-\delta}$	$(NH_4)_2Ce(NO_3)_6$ [g]	SnC_2O_4 [g]	$C_2H_5NO_2$ [g]	$PdCl_2$ [g]
SCM-A: x = 0.79	6.370	9.489	10.038	0.102
SCM-B: x = 0.99	-	12.231	10.038	0.102

4.6   Preparative synthesis of 4-Vinylphenol (2a)

For the preparation of **2a**, KPi-buffer (500 ml) was filled into a 1000 ml round bottom flask and heated to 30 °C in a water bath. Then, **1a** (0.82 g, 5.0 mmol) was added to the solution. The substrate did not dissolve entirely but the suspension was consumed during the reaction, nevertheless. Also, the double or even the quadruple amount of substrate could be used with the same setup if needed. *Bs*PAD (100 mg) was added to start the decarboxylation. The applied

enzyme was a phenolic acid decarboxylase form *Bacillus subtilis* (*Bs*PAD) and was obtained as freeze-dried cell-free extract (CFE) from the Institute of Molecular Biotechnology, TU Graz. During enzyme handling, it was important to not expose it too long to ambient conditions. Therefore, the enzyme should only be measured out after finishing all preparations and the remaining *Bs*PAD must be put back into the freezer immediately. The reaction progress was monitored visually at the beginning. The suspension should turn into a clear and slightly yellowish solution. Then, the conversion of the substrate can be determined by TLC (eluent = cyclohexane:ethyl acetate = 1:1, R_f(**1a**) = 0.36; R_f(**2a**) = 0.78) or HPLC (Method A, see section 4.12). When full conversion was reached, the intermediate **2a** was extracted with MTBE (3 x 100 ml). The organic phases were combined and washed with brine (1 x 100 ml). Further, the organic solution was dried over Na_2SO_4 and filtered into a round bottom flask with known tare value. The solvent was removed at 0 °C in a rotary evaporator by gradually reducing the pressure. Afterwards, the flask was weighted to determine the yield of **2a** and then the intermediate was dissolved in MTBE in order to obtain a 50 mM solution. The solution should be stored at 4 °C.

4.7 Heck coupling in batch

The Heck reaction and the optimization in batch for the later continuous flow reaction was the main part of this thesis. Thus, numerous different batch reactions were performed and many different process parameters were investigated. In order to keep this section in a sensible extent, a general procedure is described without explaining the exact reaction conditions. The reactions were performed within the range of values given in Table 7 for the different parameters. In chapter *3. Results and Discussion* certain experiments and the applied reaction conditions are explained in more detail for better understanding to be able to compare the findings. For the batch reactions a given amount (see Table 7) of **2a** dissolved in MTBE was filled into a 50 ml round bottom flask. The solvent was removed by a rotary evaporator using an ice bath at 0 °C and gradually reducing the pressure. The mild conditions were needed to prevent possible polymerization of the intermediate. It was also important to remove the MTBE entirely because the organic solvent would lower the activity of the Pd-catalyst later on. The remaining substrate in the flask was a slightly yellowish oil or occurs partially or fully crystalized, depending on quantity, actual bath temperature and rapidity of the solvent evaporation. In the next step, the needed volume of reaction solvent, base and **3a'** or **3b'**, respectively (see Table 7) were poured into the flask and heated to

the demanded temperature (see Table 7) in an oil bath. After a few minutes of preheating the reference sample (100 µl) was taken. Next, the prepared catalyst (see Table 7) was added by rapidly flushing the catalyst powder into the flask with a small amount of reaction solution using a pipette. At this moment the timing starts. Samples (100 µl) were taken at certain points in time and analyzed with HPLC (method B, see section 4.12).

Table 7. List of different reaction parameters investigated for the optimization of the Heck coupling of **2a** and **3a'**/**3b'**.

Reaction parameter	Investigated range	Side note
Catalyst	0.065 – 0.977 mol% Pd ref. to limiting comp.	$Pd(PPh_3)_4$ (homogeneous) KAP-Pd SCM-A/B ($Ce_{0.99-x}Sn_xPd_{0.01}O_{2-\delta}$)
Conc. 2a	10 – 200 mol/l	
Conc. 3a/3b	9.1 – 133 mol/l	
Conc. base	1.5 – 10 mol eq. ref. to limiting comp.	K_2CO_3, Na_2CO_3, NaOAc, NaOH Diisopropylethylamine (DIPEA) Tributylamine
Limiting comp.	**2a** or **3a'**/**3b'**	
Solvent system	Various mixtures and ratios of: water, EtOH, glycerol, KPi-buffer, DES(A), DES(B), DES(C), DES(D)	Not all possible variations of mixtures were used
Temperature	65 – 90 °C	

4.8 Heck coupling in continuous flow

The continuous Heck reactions of **2a** were conducted in column-S and column-L, which were packed with palladium-catalyst SCM-A ($Ce_{0.20}Sn_{0.79}Pd_{0.01}O_{2-\delta}$) according to Table 8. Behind the reactor a BPR was attached to maintain a constant pressure of 75 psi (5.17 bar) and to avoid bubble formation due to solvent evaporation. Before starting, the reactor (see Table 8) was heated to 85 °C

in a water bath and flushed with pure solvent (see Table 8). **2a**, **3a'/3b'** and K_2CO_3 were dissolved in the solvent mixture. After taking a reference sample (50 µl), the prepared stock was filled into a stainless-steel syringe and attached to a syringe pump. The experiments ran with the given flow rates in Table 8 and samples (50 µl) were taken every 15 min and analyzed by HPLC (method B, see section 4.12).

Table 8. List of conducted continuous Heck coupling of **2a** and **3a'/3b'** with K_2CO_3 as base in packed column-S and column-L (catalyst A: $Ce_{0.20}Sn_{0.79}Pd_{0.01}O_{2-\delta}$). Reaction temperature 85 °C

Exp # Reactor	Catalyst [g]	Flow rate [ml/min]	Conc. 2a / 3a'(3b') / K₂CO₃ [mmol/l]	Solvent composition [v:v:v:v]
A1 column-S	1.8	0.102	35.0 / 52.5 / 52.5	DES(A):KPi-buffer:H₂O:EtOH = 1:1:1:1
A2 column-S	1.8	0.114	10.0 / 15.0 / 52.5	DES(A):KPi-buffer:H₂O:EtOH = 1:1:1:1
A3 column-L	5.5	0.091	10.0 / 15.0 / 52.5	DES(A):KPi-buffer:H₂O:EtOH = 6:5:2.25:6.75
A4 column-L	5.5	0.097	10.0 / 9.1 / 27.3	DES(A):KPi-buffer:H₂O:EtOH = 6:5:2.25:6.75
A5 column-L	5.5	0.097	10.0 / 9.1 (**3b'**) / 27.3	DES(A):KPi-buffer:H₂O:EtOH = 6:5:2.25:6.75

4.9   Combined setups

Different approaches and reactor configurations were tried, as shown in Table 9. All experiments followed the same procedure.

First, two stock solutions were prepared. For the decarboxylation step, **1a** (see Table 10) was dissolved in DES(A):KPi-buffer = 1:1 (v:v) and for the Heck reaction a solution of **3a'** and K_2CO_3 (see Table 10) in DES(A):H₂O:EtOH = 1:2.25:6.75 (v:v:v) was prepared. Samples (50 µl) were drawn from both stocks as reference. Both flow rates of the stock solutions were equal and set to about 0.1 ml/min, giving a solvent composition in step 2 of DES(A):KPi-buffer:H₂O:EtOH =

6:5:2.25:6.75 (v:v:v:v). The exact flow rates will be mentioned in the results and discussion section. In the next step, the reactors were filled with *Bs*PAD beads (160mg *Bs*PAD in 2 % (w/v) alginate (4 ml)) and with the palladium catalyst SCM-A and then heated to reaction temperature (Decarboxylation: 30 °C; Heck: 85 °C). Afterwards, the reactors were flushed separately with the appropriate solvent mixtures. The experiments started with only running step 1 till steady-state. The reaction was monitored by taking samples (50 µl) every 15 min and analyzing them by HPLC (method A, see section 4.12). After a constant outflow of step 1 was reached, the whole setup was assembled and ran as a two-step reaction cascade. A BPR (75 psi = 5.17 bar) was used at the outlet to avoid bubble formation inside the packed column. In experiments with a CSTR used as decarboxylation reactor (see Table 9), an additional pump had to be used as the peristaltic pumps were not able to provide such high pressure levels. The outflow of step 1 and the second stock with the Heck reagents were mixed in a vial with a volume of 8 ml, from where the reaction solution was pumped into the packed column reactor by an HPLC pump. The flow rate of the HPLC pump had to match the sum of both stock pumps. Also, it is crucial to keep the fluid level in the mixing vial constant and to avoid the suction of air into the system. Air bubbles would interrupt the flow of the reaction solution through the catalyst bed, thus producing unreproducible results. The combined process was also monitored by taking samples (50 µl) every 15 min and analyzing by HPLC (method B, see section 4.12).

Table 9. Different reactor setups for the combined two-step reaction with decarboxylation and Heck reaction.

Exp. #	Pump decarbox.	Reactor decarbox.	Pump Heck	Reactor Heck
B1	Syringe pump	column-L	Syringe pump	column-S
B2	Syringe pump	2x column-S	Syringe pump	column-L
B3	Peristaltic pump	CSTR	Syringe pump + HPLC pump	column-L

Table 10. Reactant concentrations, *Bs*PAD and catalyst SCM-A amount used in the combined continuous setups

Exp. #	Conc. 1a [mmol/l]	Conc. 3a' / base [mmol/l]	SCM-A [g]
B1	20.0	30.0 / 105.0	1.8
B2	20.0	30.0 / 105.0	5.5
B3	45.0 (suspension)	49.5 / 81.9	5.5

4.10 Further substrates

4.10.1 Decarboxylation

The substrates were decarboxylated in flow to immediately test the performance under continuous reaction conditions. For this purpose, the acids were decarboxylated one after another in alphabetical order (first **1b,** last **1e**) in the same reactor with the same enzyme beads. The outflow was collected for further use.

Enzyme immobilized in alginate beads (160 mg *Bs*PAD, 2 % (w/v) sodium alginate (4 ml)) were prepared as described in section 4.4 and filled into two column-S, which served as continuous flow reactors. **1b-1e** (see Table 11) were dissolved in the appropriate volume of the solvent DES(A):KPi-buffer = 1:1 (v:v) (see Table 11). The solutions were filled into a stainless-steel syringe, which was then attached to a syringe pump. The column reactors were heated to 30 °C in a water bath and the substrates were pumped through with the flow rates given of 0.091 ml/min. After running out of substrate, the reactor was flushed with pure solvent and the outflow was collected further on to obtain the maximum amount of product for each substrate. The reaction was monitored by HPLC (Method B, see section 4.12). The products of the decarboxylation **2b-2e** were extracted with ethyl acetate (3 x 20 ml) and dried over Na_2SO_4. Afterwards, the ethyl acetate was removed under reduced pressure and the intermediates were used as such for the next reaction step.

Table 11. Amounts of **1b-1e** for the continuous decarboxylation with the appropriate volume of solvent (DES(A):KPi-buffer = 1:1(v:v)). Reaction Temp.: 30 °C; 160 mg *Bs*PAD immobilized in 80 mg alginate as beads

Substrate	Mass [mg]	Amount [mmol]	Volume [ml]
1b (3-methoxy-)	116.6	0.600	30.0
1c (3-fluoro-)	50.3	0.276	13.8
1d (3-chloro-)	61.8	0.311	15.6
1e (3-bromo-)	64.6	0.266	13.3

4.10.2 Heck reaction

Heck coupling of the synthesized intermediates **2b-2e** was performed in batch with iodobenzene **3a'** as halide coupling reagent and K_2CO_3 as base. All the obtained product from the decarboxylation (**2b-2e**) was used and dissolved in DES(A):KPi-buffer:H_2O:EtOH = 6:5:2.25:6.75 (v:v:v:v) (see Table 12) in order to obtain a concentration of about 10 mmol/l. Assuming >99% purity of **2b-2e**, **3a'** (see Table 12, 9.1 mmol/l) and K_2CO_3 were added to the reaction solution. A reference sample (100 µl) was taken after heating to 85 °C in an oil bath. The reaction was started by adding catalyst SCM-A and lasted for 4 h. Samples (100 µl) were withdrawn after 10, 20, 30, 60, 120 and 240 min and analyzed by HPLC (method B, see section 4.12).

Table 12. Reactants used for the Heck reaction of **2b-2e** with the applied amount of catalyst SCM-A and solvent (DES(A):KPi-buffer:H_2O:EtOH = 6:5:2.25:6.75 (v:v:v:v)). Reaction Temp.: 30 °C

Substrates	Iodobenzene 3a'		K_2CO_3		SCM-A		Volume
	[mg]	[mmol]	[mg]	[mmol]	[mg]	[mol%]	[ml]
2b (3-methoxy-)	24.5	0.120	37.3	0.270	12.7	0.74	12.0
2c (3-fluoro-)	32.2	0.158	37.4	0.271	12.6	0.56	18.0
2d (3-chloro-)	48.0	0.235	37.6	0.272	12.9	0.38	27.0
2e (3-bromo-)	27.2	0.133	37.5	0.271	12.5	0.66	15.0

4.11   Rearrangement reaction of 5aa' to 4aa'

To obtain representative results, the entire amount of the product mixture needed for this investigation was synthesized at once. **1a** (1366 mg, 8.32 mmol) was dispersed in KPi-buffer (500 ml) and heated to 30 °C in a water bath. Then, *Bs*PAD (107.1 mg) was added. The reaction progress was tracked till full conversion was reached by withdrawing samples (100 µl) at certain points in time and analyzed by HPLC (method A, see section 4.12). After finishing the reaction, the solution was heated to 80 °C to denature the enzyme, which then precipitated as white particles. Further the solution was filtered and the intermediate **2a** was extracted with MTBE (4 x 100 ml) and the organic phase was washed with brine (1 x 100 ml). The solvent was removed by a rotary evaporator. Afterwards, the reactants for the Heck reaction were calculated with the assumption of fully conversion in the first step. **3a'** (1724.7 mg, 8.45 mmol) and K_2CO_3 (568.4 mg, 4.11 mmol) were added to the intermediate and dissolved in DES(A):KPi-buffer:H_2O:EtOH = 6:5:2.25:6.75 (v:v:v:v) (150 ml). The solution was heated to 85 °C in an oil bath and a reference sample (100 µl) was taken. SCM-A (434.8 mg) was added and the reaction was again monitored by sampling (100 µl) after certain points in time and analyzing by HPLC (method B, see section 4.12). After full conversion of **2a**, the reaction products were extracted with MTBE (4x 100 ml) and the organic phase was washed with brine (1x 100 ml). The solvent was again removed by rotary evaporation. The product mixture was isolated by purification using flash column chromatography. EtOAc:n-hexane = 1:3 (v:v) served as eluent. R_f(**4aa'**) = 0.42; R_f(**5aa'**) = 0.51 (on TLC; eluent:EtOAc:n-hexane = 1:3 (v:v)).

Several different experiments were performed to evaluate the rearrangement reaction. The investigated reaction parameters were amounts of **4aa'** and **5aa'**, K_2CO_3 as base and SCM-A catalyst. The reactions were prepared by dissolving the synthesized product mixture **4aa'** and **5aa'** and K_2CO_3 according to the amounts given in Table 13. DES(A):KPi-buffer:H_2O:EtOH = 6:5:2.25:6.75 (v:v:v:v) (5 ml) served as reaction solution like in the Heck reactions. The temperature was also kept identical with 85 °C. After the reference sample (50 µl) was taken, catalyst SCM-A (see Table 13) was added to the solution to start the reaction. The rearrangement progress was followed by HPLC (method B, see section 4.12). Thus, samples (50 µl) were taken after 30, 60, 120 and 240 min.

Table 13. Reaction overview of the performed rearrangement reactions of **5aa'** into **4aa'**. Amounts of product mixture, base and catalyst were varied. Solvent volume and reaction temperature were constant with 5 ml and 85 °C, respectively.

Exp #	4aa' + 5aa'		K_2CO_3		SCM-A	
	[mg]	[mmol]	[mg]	[mmol]	[mg]	[mol%]
C1	50.0	0.255	0.0	0	50.0	1.4
C2	25.0	0.127	18.8	0.136	25.0	1.4
C3	25.0	0.127	37.7	0.273	25.0	1.4
C4	10.0	0.051	18.8	0.136	10.0	1.4
C5	10.0	0.051	18.8	0.136	25.0	3.4

4.12   Analysis method

Evaluation of the experiments was performed by HPLC measurements. An Agilent 1100 series HPLC system equipped with online degasser, quaternary pump, autosampler, thermostated column compartment, ThermoFisher Scientific Accucore™ C18 reversed phase column (50 x 4.6 mm; 2.6 µm) and UV-visible diode array detector was used. Methanol and buffer ($H_2O:H_3PO_4$ = 300:1 (v:v)) served as eluents and depending on the experiment and chemical components different methods were applied. The samples were diluted 100:1100 µl for batch and 50:550 µl for continuous experiments.

The HPLC methods used are depicted in Table 14.

Table 14. HPLC methods used for measurements

Method	MeOH [v/v]	Buffer [v/v]	Gradient [min]	Total run time [min]	Total flow rate [ml/min]
A	40	60	-	5	1
	40	60	1		
B	90	10	12	16	1
	40	60	14		

5   Conclusion and Outlook

The goal of this thesis was to develop an integrated chemo-enzymatic reaction cascade in continuous flow for the synthesis of resveratrol derivatives. For this purpose, several parameters were optimized in batch before further enhancing the reaction conditions in flow experiments.

At the beginning, a suitable (bio-)catalyst had to be found for the two-step reaction. From previous works by Schweiger *et al.*[60] it was known that phenolic acid decarboxylase from *Bacillus subtilis* (*Bs*PAD) is a well performing enzyme for the decarboxylation of *p*-coumaric acid and its derivatives. Hence, *Bs*PAD was chosen as biocatalyst which was immobilized in alginate beads for the application in continuous flow. For the Heck reaction three different heterogeneous catalysts with organic and inorganic support were tested. SCM-A ($Ce_{0.20}Sn_{0.79}Pd_{0.01}O_{2-\delta}$), a cerium-tin-oxide supported palladium catalyst, emerged as best choice for the intended setup with fast conversion of the substrates and only little leaching.

In the next step, the effects of the reaction temperatures were investigated. Again, it was known that the optimal reaction temperature for the enzyme is 30 °C, thus this temperature was fixed for the decarboxylation step without further experiments. However, several Heck couplings were conducted in batch in order to find the right temperature for the second reaction step in the sequence. Eventually, applying 85 °C was found to be the best course of action as the reaction rate is already high enough giving good conversion and yield in a reasonable amount of time. Moreover, this temperature is still low enough to avoid evaporation of the solvent and the CO_2 formed by the decarboxylation is still soluble in the used solvent system. This way, bubble-free processing was ensured which was crucial as bubbles in the catalyst bed would drastically disturb the material flow through the reactor and cause a severe decrease of the reaction performance.

Another parameter to set for the reaction system is the composition of the solvent in each reaction step. As found by Schweiger, a deep eutectic solvent (DES)/buffer mixture 1:1 (v:v) is a suitable solvent for the decarboxylation. Several tests with different DES were conducted and it was confirmed that the DES(A) comprising ChCl and glycerol in a molar ratio of 1:2 is the best choice for the enzymatic step, as shown by Schweiger. In order to overcome the problem of dissolving an aryl halide and an inorganic base in the same stock, DES(A) was added to a water-ethanol mixture in an extent of 10 %. This gives a composition of DES(A):H_2O:EtOH = 1:2.25:6.75 (v:v:v) in the

Heck reactant stock and a final composition of DES(A):KPi-buffer:H$_2$O:EtOH = 6:5:2.25:6.75 (v:v:v:v) in the packed bed reactor.

As the Heck coupling requires a basic milieu, the influence of the type and amount of base was investigated as well. It was shown that the basicity parameter has a great impact on the outcome of the reaction. Inorganic bases were found to generally perform better than the tested organic counterparts in this particular system. K$_2$CO$_3$ and Na$_2$CO$_3$ showed the similar performances with the Na$_2$CO$_3$ being even little better but, nevertheless, K$_2$CO$_3$ was chosen as base because of the much higher solubility. Ensuring homogeneous flow without precipitation or liquid phase separation seemed more important than slightly higher conversion and yield.

The influence of the substrate concentration and the reactant excess was investigated in batch and in continuous flow reactions. Different approaches with either the vinyl component **2** or the aryl halide **3** in excess were tested. Ultimately, it was decided to use a setup with the aryl halide being in excess by 1.1 mol eq. referring to the vinyl component. The concentration in the system was limited by the solubility of the phenolic acids **1**. Even though, the solubility was enhanced by the application of DES(A) in comparison to neat buffer, not more than 20 mmol/l of the substrate were soluble.

With all these optimizations, it was possible to develop two different integrated continuous flow setups. Parts of these results were published by Grabner and co-workers.[1] One approach with packed bed reactors in both steps was successfully operated for almost 24 h. The reaction was performed with a 20 mmol/l solution of *p*-coumaric acid (**1a**) and an average yield of 21 % and a product (**4aa'**) concentration of 2.3 mmol/l were achieved. In another setup a 3D-printed CSTR for the enzymatic decarboxylation and a packed bed reactor for the Heck coupling was used. The CSTR allowed the application of a substrate suspension with a loading of 45 mmol/l and it was possible to increase the product concentration to 3.2 mmol/l. Unfortunately, the yield relative to the substrate becomes lower at higher overall concentration. Thus, only about 15 % could be reached. All in all, it was shown that the yield hardly ever exceeds 25 % no matter what adjustments were made in batch and in continuous flow. It seems that the thermodynamic equilibrium of the reaction simply does not allow the product formation above a certain value. Moreover, side reactions of the educts were observed, namely polymerization of the vinyl

component and homo-coupling of the aryl halide. These side reactions further lower the formation of the desired product.

Besides the long-term continuous flow experiments with *p*-coumaric acid **1a** as substrate and iodobenzene (**3a'**) as coupling reactant other tests with derivatives of *p*-coumaric acid (**1b**-**1e**) and 4-iodophenol (**3b'**) were conducted and served as proof of concept for the applicability of these reagents in the final setups. The substituted phenolic acids (**1b**-**1e**) were decarboxylated in continuous flow using a packed bed reactor after which the intermediate vinyl components (**2b**-**2e**) were isolated for a Heck coupling with **3a'** in batch. Furthermore, Heck reactions in batch and continuous flow with 4-vinylphenol (**2a**) and 4-iodophenol **3b'** were successfully conducted. This way it was possible to proof the feasibility of the synthesis of different products with the developed setup.

In the course of performing Heck reactions, it was observed that the ratio between desired product **4aa'** and the side product **5aa'** changes over time in favor of **4aa'**. Thus, several experiments were performed where the isolated product mixture was stirred at usual Heck coupling conditions. It was discovered that a rearrangement reaction from **5aa'** to **4aa'** takes place by a migration of one of the phenyl groups to form the corresponding stilbene. Due to time limitation this phenomenon was not further investigated but it shows a potential way of increasing the product yield and the selectivity of the reaction sequence.

As a short outlook, some ideas to further improve on the findings of this thesis should be mentioned. On the one hand, one approach would be to further increase the reaction temperature. This could be achieved by changing the solvent composition, e.g. using more or another type of DES. Another way would be to apply higher backpressures in the flow setups and this way prevent the formation of bubbles in the reactors at higher temperature. A higher reaction temperature would most likely improve the yield and selectivity as it was observed in the test described in section 3.2. On the other hand, it can be considered to disconnect the two reaction steps and run them separately. The enzymatic already operates at fast conversion and high yield but the Heck reaction appears to be the big challenge. By disconnecting the reaction steps, the Heck reaction could be optimized separately. For example, a new solvent system with other DES could be tried and also one would not have to worry about the influence of the buffer and the dissolved CO_2 from the first

step. Also, the phenolic groups of the intermediate product could be protected before the Heck reaction, as this increases the yield of the desired coupling product.

6 Appendix

6.1 Setup images
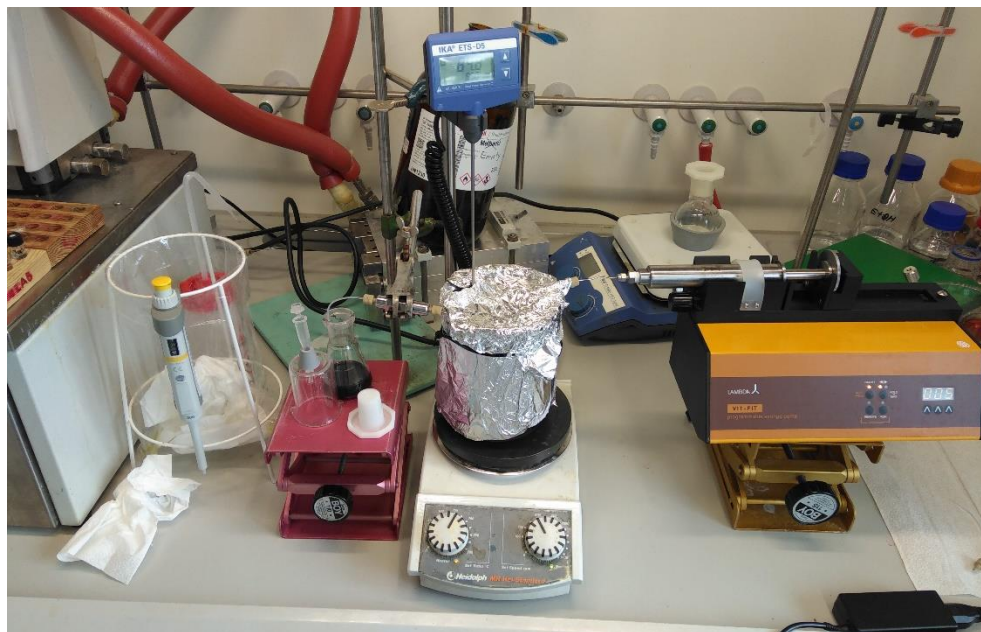
Figure A 1. Setup for continuous Heck reaction. Experiment A1 - A5
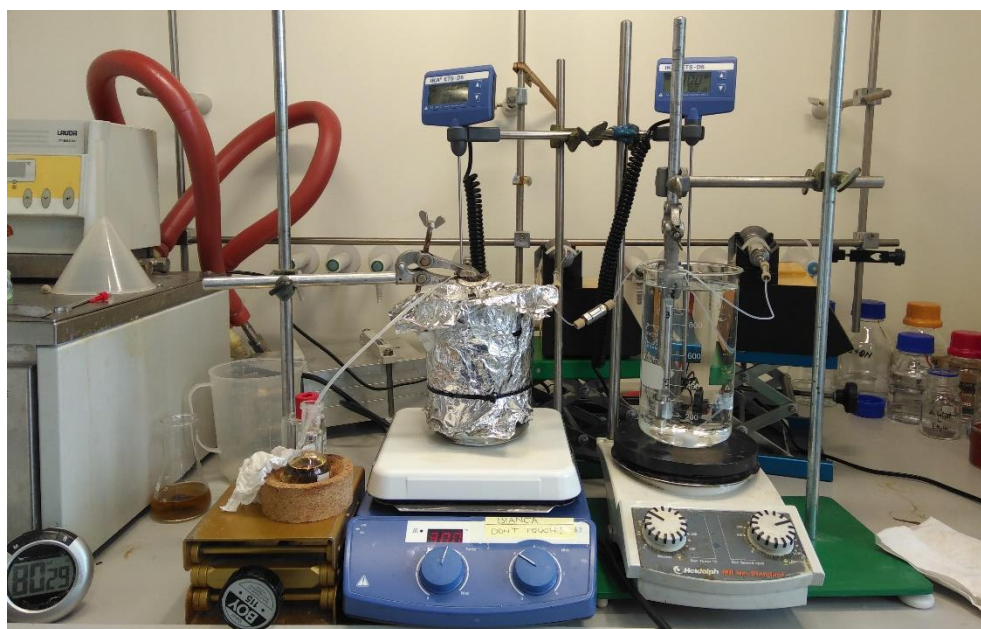
Figure A 2. Combined reaction setup of experiment B1. Decarboxylation in column-L and Heck coupling in column-S

Figure A 3. Packed column-L for Heck reactions in combined setups (experiment B2 and B3) with T-mixer
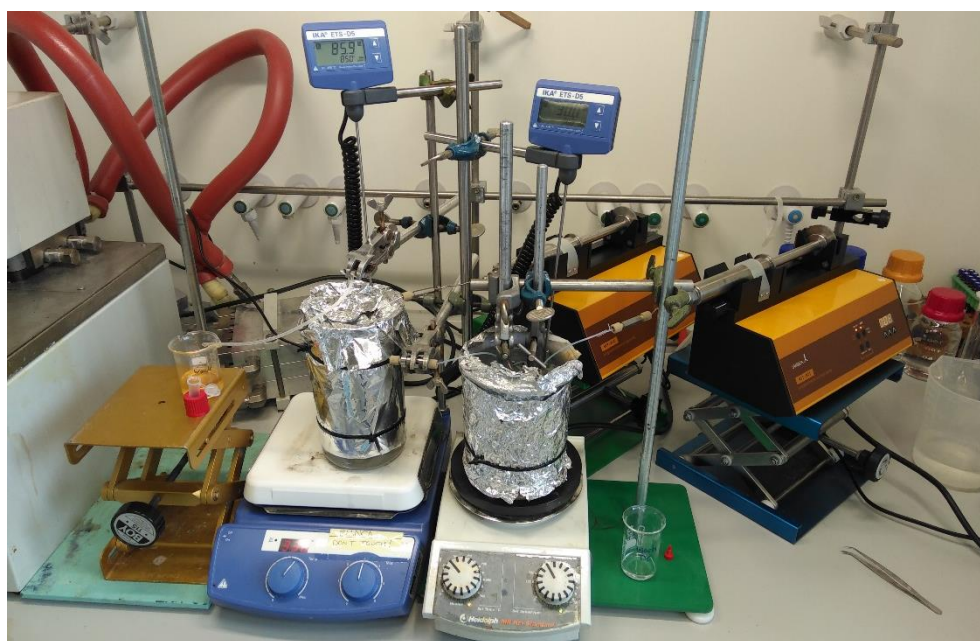
Figure A 4. Combined reaction setup of experiment B2. Decarboxylation in 2 x column-S and Heck coupling in column-L

Figure A 5. Combined reaction setup of experiment B3. Decarboxylation in CSTR and Heck coupling in column-L

6.2 NMR

NMR-measurements were recorded using a Bruker Avance III 300 MHz spectrometer in CDCl$_3$. ^{1}H-NMR of **4aa'** and **5aa'** shown in Figure A 6 and Figure A 7, respectively.

4-Hydroxystilbene (4aa'): ^{1}H-NMR: 7.50 – 7-48 (d, 2H, Ar-H), 7.43 - 7.40 (d, 2H, Ar-H), 7.37 - 7.32 (t, 2H, Ar-H), 7.26 - 7.22 (t, 1H, Ar-H), 7.09 - 6.94 (dd, 2H, H-C=C-H), 6.85 – 6.82 (d, 2H, Ar-H), 4.77 (s, 1H, O-H) ppm.

4-(1-phenylvinyl) phenol (5aa'): ^{1}H-NMR: 7.31 – 7.28 (m, 5H, Ar-H), 7.25 - 7.20 (d, 2H, Ar-H), 6.81 - 6.78 (d, 2H, Ar-H), 5.39 (s, 1H, C=C-H), 5.35 (s, 1H, C=C-H), 4.74 (s, 1H, O-H) ppm.
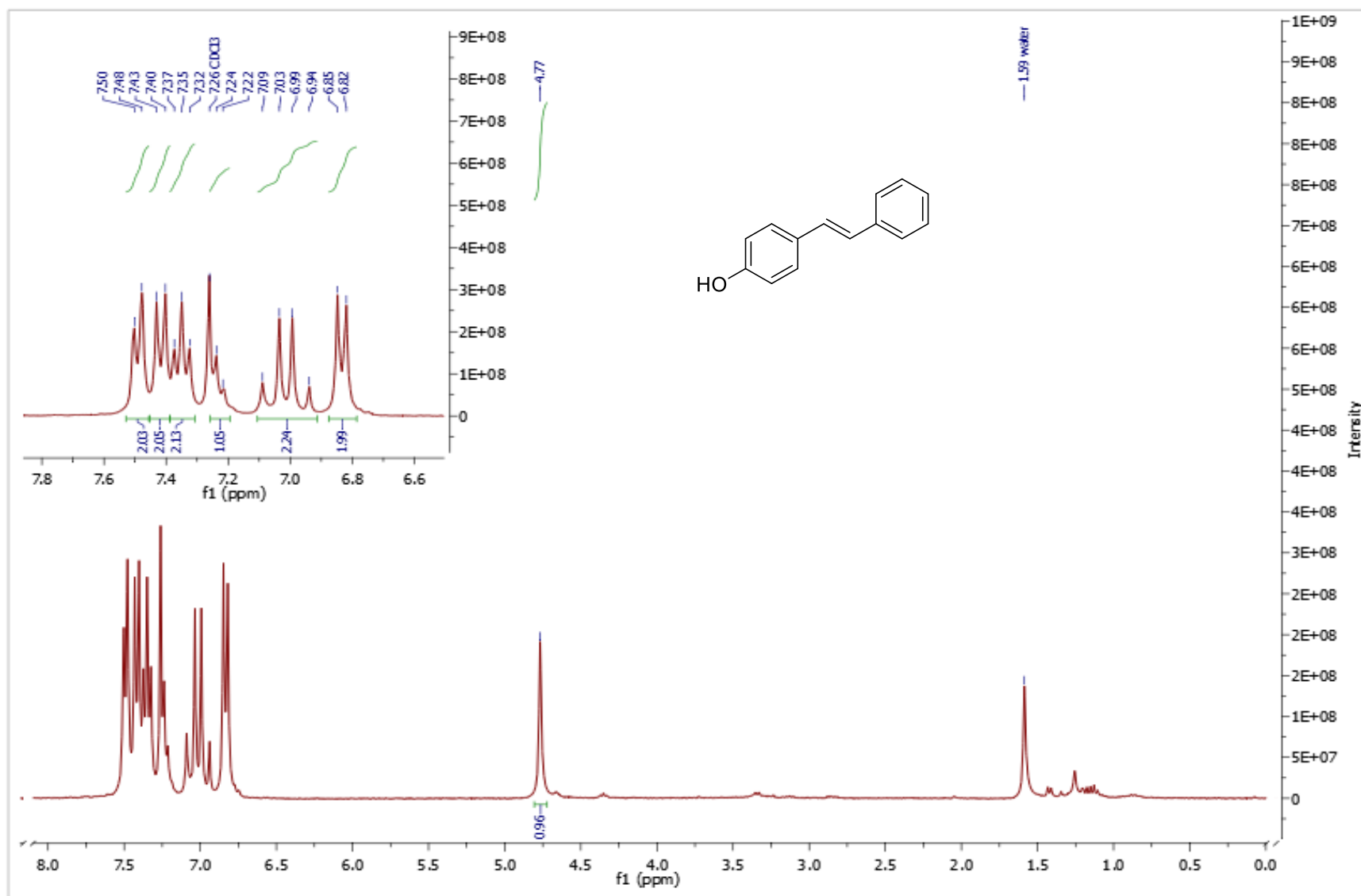
Figure A 6. ^{1}H NMR of **4aa'**
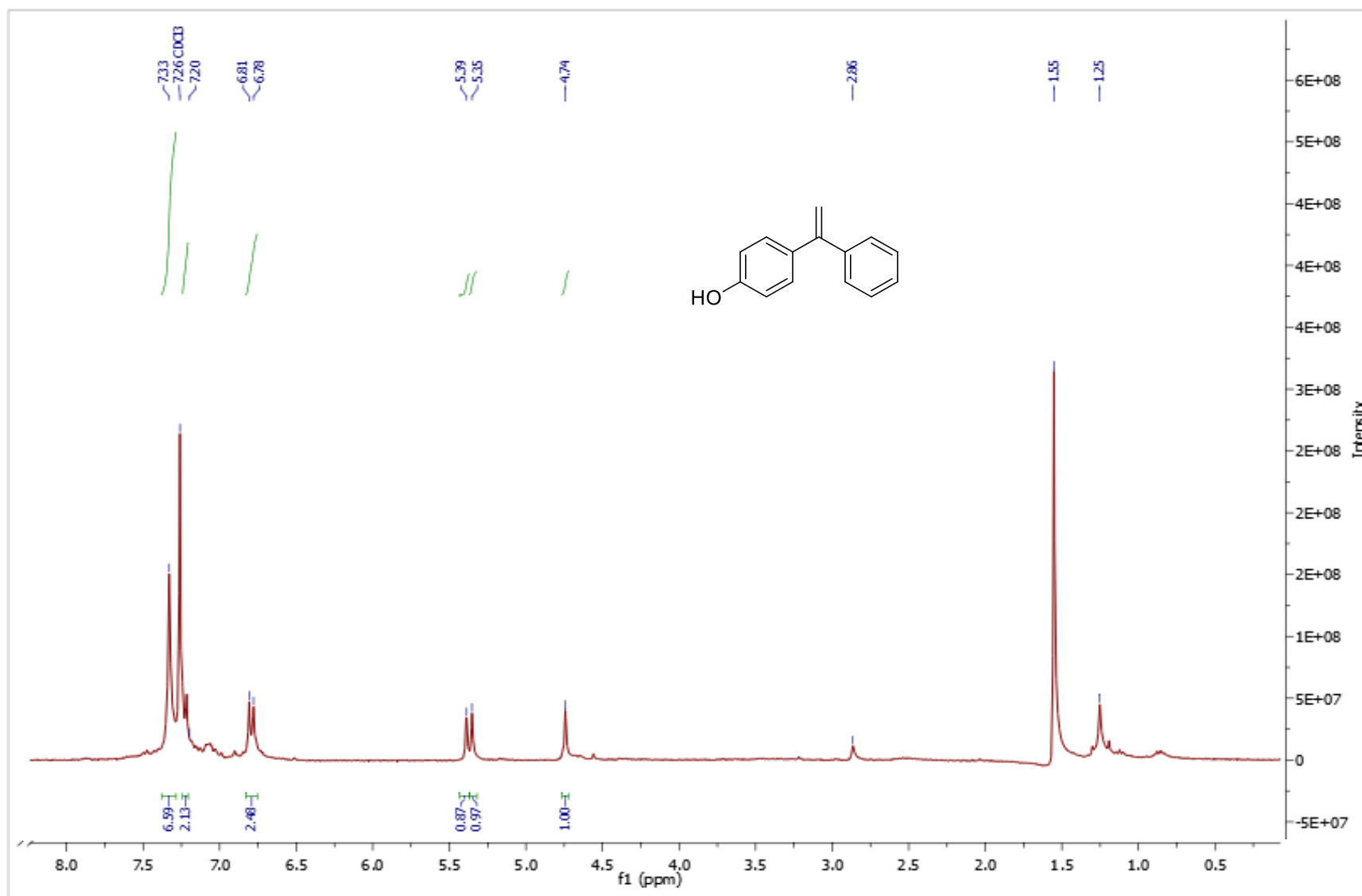
Figure A 7. ^{1}H NMR of **5aa'**

7   Abbreviations and Symbol Directory

%gain$_t$	Gain of HPLC area ratio of **4aa'** to **5aa'** after a certain reaction time
A$_{4aa'}$, A$_{5aa'}$	HPLC peak area of **4aa'** and **5aa'**
API	Active pharmaceutical ingredient
AR$_t$	HPLC area ratio of **4aa'** to **5aa'** after a certain reaction time
ArX	Aryl halide
BPR	Back pressure regulator
BsPAD	Phenolic acid decarboxylase from *Bacillus subtilis*
CFE	Cell-free extract
ChCl	Choline chloride
CSTR	Continuous stirred tank reactor
DES	Deep eutectic solvent
DIPEA	Diisopropylethylamine
DPI	Dots per inch
EtOAc	Ethyl acetate
EtOH	Ethanol
HBD	Hydrogen bond donator
HPLC	High performance liquid chromatography
KAP	Knitting aryl network Polymer
KPi-buffer	Potassium phosphate buffer
LCD	Liquid crystal chromatography
MTBE	Methyl *tert*. butyl ether
NADES	Natural deep eutectic solvent

OTf	Triflate ($CF_3SO_3^-$, trifluoromethanesulfonate)
QAS	Quaternary ammonium salt
SCM	Solution combustion method
SLA	stereolithography apparatus
TLC	Thin layer chromatography

8   List of Figures

9   List of Schemes

10   List of Tables

11   Bibliography

(1)   Grabner, B.; Schweiger, A. K.; Gavric, K.; Kourist, R.; Gruber-Wölfler, H. Rsc.Li/Reaction-Engineering. *React. Chem. Eng.* **2020**, *1*. https://doi.org/10.1039/C9RE00467J.

(2)   Nivelle, L.; Hubert, J.; Courot, E.; Jeandet, P.; Aziz, A.; Nuzillard, J.-M.; Renault, J.-H.; Clément, C.; Martiny, L.; Delmas, D.; et al. Anti-Cancer Activity of Resveratrol and Derivatives Produced by Grapevine Cell Suspensions in a 14 L Stirred Bioreactor. *Molecules* **2017**, *22* (3), 474. https://doi.org/10.3390/molecules22030474.

(3)   El Sohly, M.; Gul, W.; Cole, J. Resveratrol Esters. US 10,099,995 B2, 2014.

(4)   Aggarwal, B. B.; Bhardwaj, A.; Aggarwal, R. S.; Seeram, N. P.; Shishodia, S.; Takada, Y. Role of Resveratrol in Prevention and Therapy of Cancer: Preclinical and Clinical Studies. *Anticancer Research*. September 2004, pp 2783–2840.

(5)   Paller, C. J.; Rudek, M. A.; Zhou, X. C.; Wagner, W. D.; Hudson, T. S.; Anders, N.; Hammers, H. J.; Dowling, D.; King, S.; Antonarakis, E. S.; et al. A Phase i Study of Muscadine Grape Skin Extract in Men with Biochemically Recurrent Prostate Cancer: Safety, Tolerability, and Dose Determination. *Prostate* **2015**, *75* (14), 1518–1525. https://doi.org/10.1002/pros.23024.

(6)   Howells, L. M.; Berry, D. P.; Elliott, P. J.; Jacobson, E. W.; Hoffmann, E.; Hegarty, B.; Brown, K.; Steward, W. P.; Gescher, A. J. Phase I Randomized, Double-Blind Pilot Study of Micronized Resveratrol (SRT501) in Patients with Hepatic Metastases - Safety, Pharmacokinetics, and Pharmacodynamics. *Cancer Prev. Res.* **2011**, *4* (9), 1419–1425. https://doi.org/10.1158/1940-6207.CAPR-11-0148.

(7)   Zhu, W.; Qin, W.; Zhang, K.; Rottinghaus, G. E.; Chen, Y. C.; Kliethermes, B.; Sauter, E. R. Trans -Resveratrol Alters Mammary Promoter Hypermethylation in Women at Increased Risk for Breast Cancer. *Nutr. Cancer* **2012**, *64* (3), 393–400. https://doi.org/10.1080/01635581.2012.654926.

(8)   Rodríguez-Enríquez, S.; Pacheco-Velázquez, S. C.; Marín-Hernández, Á.; Gallardo-Pérez, J. C.; Robledo-Cadena, D. X.; Hernández-Reséndiz, I.; García-García, J. D.; Belmont-Díaz, J.; López-Marure, R.; Hernández-Esquivel, L.; et al. Resveratrol Inhibits Cancer Cell Proliferation by Impairing Oxidative Phosphorylation and Inducing Oxidative Stress. *Toxicol. Appl. Pharmacol.* **2019**, *370*, 65–77. https://doi.org/10.1016/j.taap.2019.03.008.

(9)   Diaz-Gerevini, G. T.; Repossi, G.; Dain, A.; Tarres, M. C.; Das, U. N.; Eynard, A. R. Beneficial Action of Resveratrol: How and Why? *Nutrition*. Elsevier Inc. February 1, 2016, pp 174–178. https://doi.org/10.1016/j.nut.2015.08.017.

(10)   Tang, Y. W.; Shi, C. J.; Yang, H. L.; Cai, P.; Liu, Q. H.; Yang, X. L.; Kong, L. Y.; Wang, X. B. Synthesis and Evaluation of Isoprenylation-Resveratrol Dimer Derivatives against Alzheimer's Disease. *Eur. J. Med. Chem.* **2019**, *163*, 307–319. https://doi.org/10.1016/j.ejmech.2018.11.040.

(11)   Öztürk, E.; Arslan, A. K. K.; Yerer, M. B.; Bishayee, A. Resveratrol and Diabetes: A Critical Review of Clinical Studies. *Biomedicine and Pharmacotherapy*. Elsevier Masson SAS November 1, 2017, pp 230–234. https://doi.org/10.1016/j.biopha.2017.08.070.

(12)   Chen, S.; Zhao, X.; Ran, L.; Wan, J.; Wang, X.; Qin, Y.; Shu, F.; Gao, Y.; Yuan, L.; Zhang, Q.; et al. Resveratrol Improves Insulin Resistance, Glucose and Lipid Metabolism in Patients with Non-Alcoholic Fatty Liver Disease: A Randomized Controlled Trial. *Dig. Liver Dis.* **2015**, *47* (3), 226–232. https://doi.org/10.1016/j.dld.2014.11.015.

(13)   de Ligt, M.; Timmers, S.; Schrauwen, P. Resveratrol and Obesity: Can Resveratrol Relieve Metabolic Disturbances? *Biochimica et Biophysica Acta - Molecular Basis of Disease*. Elsevier B.V. June 1, 2015, pp 1137–1144. https://doi.org/10.1016/j.bbadis.2014.11.012.

(14)   Stokes, G. J. C.; Barics, S. J. A. Process for Making a Container with a Resveratrol Layer. US 10,207,291 B2.

(15)   Solladié, G.; Pasturel-Jacopé, Y.; Maignan, J. A Re-Investigation of Resveratrol Synthesis

by Perkins Reaction. Application to the Synthesis of Aryl Cinnamic Acids. *Tetrahedron* **2003**, *59* (18), 3315–3321. https://doi.org/10.1016/S0040-4020(03)00405-8.

(16) Nicotra, S.; Cramarossa, M. R.; Mucci, A.; Pagnoni, U. M.; Riva, S.; Forti, L. Biotransformation of Resveratrol: Synthesis of Trans-Dehydrodimers Catalyzed by Laccases from Myceliophtora Thermophyla and from Trametes Pubescens. *Tetrahedron* **2004**, *60* (3), 595–600. https://doi.org/10.1016/j.tet.2003.10.117.

(17) Snyder, S. A.; Gollner, A.; Chiriac, M. I. Regioselective Reactions for Programmable Resveratrol Oligomer Synthesis. *Nature* **2011**, *474* (7352), 461–466. https://doi.org/10.1038/nature10197.

(18) Heck, R. F.; Nolley, J. P. Palladium-Catalyzed Vinylic Hydrogen Substitution Reactions with Aryl, Benzyl, and Styryl Halides. *J. Org. Chem.* **1972**, *37* (14), 2320–2322. https://doi.org/10.1021/jo00979a024.

(19) The Nobel Prize in Chemistry https://www.nobelprize.org/prizes/chemistry/ (accessed Dec 17, 2019).

(20) Biffis, A.; Zecca, M.; Basato, M. Palladium Metal Catalysts in Heck C-C Coupling Reactions. *J. Mol. Catal. A Chem.* **2001**, *173* (1–2), 249–274. https://doi.org/10.1016/S1381-1169(01)00153-4.

(21) Heck Reaction https://www.organic-chemistry.org/namedreactions/heck-reaction.shtm (accessed Dec 17, 2019).

(22) Biffis, A.; Centomo, P.; Zotto, A. Del; Zecca, M. Pd Metal Catalysts for Cross-Couplings and Related Reactions in the 21st Century: A Critical Review. **2018**. https://doi.org/10.1021/acs.chemrev.7b00443.

(23) Schmidt, A. F.; Kurokhtina, A. A.; Larina, E. V. Simple Kinetic Method for Distinguishing between Homogeneous and Heterogeneous Mechanisms of Catalysis, Illustrated by the Example of "Ligand-Free" Suzuki and Heck Reactions of Aryl Iodides and Aryl Bromides. *Kinet. Catal.* **2012**, *53* (1), 84–90. https://doi.org/10.1134/S0023158412010107.

(24) Schmidt, A. F.; Kurokhtina, A. A. Distinguishing between the Homogeneous and Heterogeneous Mechanisms of Catalysis in the Mizoroki-Heck and Suzuki-Miyaura Reactions: Problems and Prospects. *Kinetics and Catalysis*. November 2012, pp 714–730.

https://doi.org/10.1134/S0023158412060109.

(25) Huang, L.; Wong, P. K.; Tan, J.; Ang, T. P.; Wang, Z. Studies on the Nature of Catalysis: Suppression of the Catalytic Activity of Leached Pd by Supported Pd Particles during the Heck Reaction. *J. Phys. Chem. C* **2009**, *113* (23), 10120–10130. https://doi.org/10.1021/jp811188f.

(26) Reimann, S.; Stötzel, J.; Frahm, R.; Kleist, W.; Grunwaldt, J. D.; Baiker, A. Identification of the Active Species Generated from Supported Pd Catalysts in Heck Reactions: An in Situ Quick Scanning EXAFS Investigation. *J. Am. Chem. Soc.* **2011**, *133* (11), 3921–3930. https://doi.org/10.1021/ja108636u.

(27) Pryjomska-Ray, I.; Gniewek, A.; Trzeciak, A. M.; Ziółkowski, J. J.; Tylus, W. Homogeneous/Heterogeneous Palladium Based Catalytic System for Heck Reaction. the Reversible Transfer of Palladium between Solution and Support. In *Topics in Catalysis*; 2006; Vol. 40, pp 173–184. https://doi.org/10.1007/s11244-006-0119-1.

(28) Cantillo, D.; Kappe, C. O. Immobilized Transition Metals as Catalysts for Cross-Couplings in Continuous Flow-A Critical Assessment of the Reaction Mechanism and Metal Leaching. *ChemCatChem* **2014**, *6* (12), 3286–3305. https://doi.org/10.1002/cctc.201402483.

(29) Kourist, R.; Guterl, J.-K.; Miyamoto, K.; Sieber, V. Enzymatic Decarboxylation-An Emerging Reaction for Chemicals Production from Renewable Resources. *ChemCatChem* **2014**, *6* (3), 689–701. https://doi.org/10.1002/cctc.201300881.

(30) Frank, A.; Eborall, W.; Hyde, R.; Hart, S.; Turkenburg, J. P.; Grogan, G. Mutational Analysis of Phenolic Acid Decarboxylase from Bacillus Subtilis (BsPAD), Which Converts Bio-Derived Phenolic Acids to Styrene Derivatives. *Catal. Sci. Technol.* **2012**, *2* (8), 1568–1574. https://doi.org/10.1039/c2cy20015e.

(31) Maeda, M.; Tokashiki, M.; Tokashiki, M.; Uechi, K.; Ito, S.; Taira, T. Characterization and Induction of Phenolic Acid Decarboxylase from Aspergillus Luchuensis. *J. Biosci. Bioeng.* **2018**, *126* (2), 162–168. https://doi.org/10.1016/j.jbiosc.2018.02.009.

(32) Schwarz, K. J.; Boitz, L. I.; Methner, F.-J. Enzymatic Formation of Styrene during Wheat Beer Fermentation Is Dependent on Pitching Rate and Cinnamic Acid Content. *J. Inst. Brew.* **2012**, *118* (3), 280–284. https://doi.org/10.1002/jib.41.

(33) Norppa, H.; Vainio, H. Genetic Toxicity of Styrene and Some of Its Derivatives. *Scandinavian Journal of Work, Environment & Health*. Scandinavian Journal of Work, Environment & HealthFinnish Institute of Occupational HealthDanish National Research Centre for the Working EnvironmentNorwegian National Institute of Occupational Health pp 108–114. https://doi.org/10.2307/40964387.

(34) Rodríguez, H.; Angulo, I.; de las Rivas, B.; Campillo, N.; Páez, J. A.; Muñoz, R.; Mancheño, J. M. *P* -Coumaric Acid Decarboxylase from *Lactobacillus Plantarum* : Structural Insights into the Active Site and Decarboxylation Catalytic Mechanism. *Proteins Struct. Funct. Bioinforma.* **2010**, NA-NA. https://doi.org/10.1002/prot.22684.

(35) Mohamad, N. R.; Marzuki, N. H. C.; Buang, N. A.; Huyop, F.; Wahab, R. A. An Overview of Technologies for Immobilization of Enzymes and Surface Analysis Techniques for Immobilized Enzymes. *Biotechnol. Biotechnol. Equip.* **2015**, *29* (2), 205–220. https://doi.org/10.1080/13102818.2015.1008192.

(36) Brena, B. M.; Batista-Viera, F. Immobilization of Enzymes; 2006; pp 15–30. https://doi.org/10.1007/978-1-59745-053-9_2.

(37) Funami, T.; Fang, Y.; Noda, S.; Ishihara, S.; Nakauma, M.; Draget, K. I.; Nishinari, K.; Phillips, G. O. Rheological Properties of Sodium Alginate in an Aqueous System during Gelation in Relation to Supermolecular Structures and Ca2+ Binding. *Food Hydrocoll.* **2009**, *23* (7), 1746–1755. https://doi.org/10.1016/j.foodhyd.2009.02.014.

(38) Martău, G. A.; Mihai, M.; Vodnar, D. C. The Use of Chitosan, Alginate, and Pectin in the Biomedical and Food Sector—Biocompatibility, Bioadhesiveness, and Biodegradability. *Polymers (Basel).* **2019**, *11* (11), 1837. https://doi.org/10.3390/polym11111837.

(39) Gutmann, B.; Cantillo, D.; Kappe, C. O. Continuous-Flow Technology - A Tool for the Safe Manufacturing of Active Pharmaceutical Ingredients. *Angewandte Chemie - International Edition*. Wiley-VCH Verlag June 1, 2015, pp 6688–6728. https://doi.org/10.1002/anie.201409318.

(40) Gutmann, B.; Kappe, C. O. Forbidden Chemistries — Paths to a Sustainable Future Engaging Continuous Processing. *J. Flow Chem.* **2017**, *7* (3–4), 65–71. https://doi.org/10.1556/1846.2017.00009.

(41)   Harper, K. C.; Moschetta, E. G.; Bordawekar, S. V.; Wittenberger, S. J. A Laser Driven Flow Chemistry Platform for Scaling Photochemical Reactions with Visible Light. *ACS Cent. Sci.* **2019**, *5* (1), 109–115. https://doi.org/10.1021/acscentsci.8b00728.

(42)   Plutschack, M. B.; Us Pieber, B.; Gilmore, K.; Seeberger, P. H. The Hitchhiker's Guide to Flow Chemistry ‖. **2017**. https://doi.org/10.1021/acs.chemrev.7b00183.

(43)   Baumann, M.; Baxendale, I. R. The Synthesis of Active Pharmaceutical Ingredients (APIs) Using Continuous Flow Chemistry. *Beilstein J. Org. Chem* **2015**, *11*, 1194–1219. https://doi.org/10.3762/bjoc.11.134.

(44)   Dallinger, D.; Kappe, C. O. Why Flow Means Green – Evaluating the Merits of Continuous Processing in the Context of Sustainability. *Current Opinion in Green and Sustainable Chemistry*. Elsevier B.V. October 1, 2017, pp 6–12. https://doi.org/10.1016/j.cogsc.2017.06.003.

(45)   Fanelli, F.; Parisi, G.; Degennaro, L.; Luisi, R. Contribution of Microreactor Technology and Flow Chemistry to the Development of Green and Sustainable Synthesis. *Beilstein J. Org. Chem* **2017**, *13*, 520–542. https://doi.org/10.3762/bjoc.13.51.

(46)   Sperl, J. M.; Carsten, J. M.; Guterl, J.-K.; Lommes, P.; Sieber, V. Reaction Design for the Compartmented Combination of Heterogeneous and Enzyme Catalysis. *ACS Catal.* **2016**, *6* (10), 6329–6334. https://doi.org/10.1021/acscatal.6b01276.

(47)   Farkas, E.; Oláh, M.; Földi, A.; Kóti, J.; Éles, J.; Nagy, J.; Gal, C. A.; Paizs, C.; Hornyánszky, G.; Poppe, L. Chemoenzymatic Dynamic Kinetic Resolution of Amines in Fully Continuous-Flow Mode. *Org. Lett.* **2018**, *20* (24), 8052–8056. https://doi.org/10.1021/acs.orglett.8b03676.

(48)   Peng, M.; Mittmann, E.; Wenger, L.; Hubbuch, J.; Engqvist, M. K. M.; Niemeyer, C. M.; Rabe, K. S. 3D-Printed Phenacrylate Decarboxylase Flow Reactors for the Chemoenzymatic Synthesis of 4-Hydroxystilbene. *Chem. – A Eur. J.* **2019**, chem.201904206. https://doi.org/10.1002/chem.201904206.

(49)   Abbott, A. P.; Capper, G.; Davies, D. L.; Munro, H. L.; Rasheed, R. K.; Tambyrajah, V. Preparation of Novel, Moisture-Stable, Lewis-Acidic Ionic Liquids Containing Quaternary Ammonium Salts with Functional Side Chains. *Chem. Commun.* **2001**, *1* (19), 2010–2011.

https://doi.org/10.1039/b106357j.

(50) Abbott, A. P.; Capper, G.; Davies, D. L.; Rasheed, R. K.; Tambyrajah, V. Novel Solvent Properties of Choline Chloride/Urea Mixtures. *Chem. Commun.* **2003**, *9* (1), 70–71. https://doi.org/10.1039/b210714g.

(51) Smith, E. L.; Abbott, A. P.; Ryder, K. S. Deep Eutectic Solvents (DESs) and Their Applications. *Chemical Reviews*. American Chemical Society November 12, 2014, pp 11060–11082. https://doi.org/10.1021/cr300162p.

(52) Abbott, A. P.; Barron, J. C.; Ryder, K. S.; Wilson, D. Eutectic-Based Ionic Liquids with Metal-Containing Anions and Cations. *Chem. - A Eur. J.* **2007**, *13* (22), 6495–6501. https://doi.org/10.1002/chem.200601738.

(53) Dai, Y.; van Spronsen, J.; Witkamp, G. J.; Verpoorte, R.; Choi, Y. H. Natural Deep Eutectic Solvents as New Potential Media for Green Technology. *Anal. Chim. Acta* **2013**, *766*, 61–68. https://doi.org/10.1016/j.aca.2012.12.019.

(54) Zhao, H.; Baker, G. A. Ionic Liquids and Deep Eutectic Solvents for Biodiesel Synthesis: A Review. *J. Chem. Technol. Biotechnol.* **2013**, *88* (1), 3–12. https://doi.org/10.1002/jctb.3935.

(55) Shishov, A.; Bulatov, A.; Locatelli, M.; Carradori, S.; Andruch, V. Application of Deep Eutectic Solvents in Analytical Chemistry. A Review. *Microchemical Journal*. Elsevier Inc. November 1, 2017, pp 33–38. https://doi.org/10.1016/j.microc.2017.07.015.

(56) Zainal-Abidin, M. H.; Hayyan, M.; Hayyan, A.; Jayakumar, N. S. New Horizons in the Extraction of Bioactive Compounds Using Deep Eutectic Solvents: A Review. *Analytica Chimica Acta*. Elsevier B.V. August 1, 2017, pp 1–23. https://doi.org/10.1016/j.aca.2017.05.012.

(57) Durand, E.; Lecomte, J.; Villeneuve, P. Deep Eutectic Solvents: Synthesis, Application, and Focus on Lipase-Catalyzed Reactions. *Eur. J. Lipid Sci. Technol.* **2013**, *115* (4), 379–385. https://doi.org/10.1002/ejlt.201200416.

(58) Ghaedi, H.; Ayoub, M.; Sufian, S.; Shariff, A. M.; Hailegiorgis, S. M.; Khan, S. N. CO2 Capture with the Help of Phosphonium-Based Deep Eutectic Solvents. *J. Mol. Liq.* **2017**, *243*, 564–571. https://doi.org/10.1016/j.molliq.2017.08.046.

(59)   Nkuku, C. A.; LeSuer, R. J. Electrochemistry in Deep Eutectic Solvents. *J. Phys. Chem. B* **2007**, *111* (46), 13271–13277. https://doi.org/10.1021/jp075794j.

(60)   Schweiger, A. K.; Winkler, C. K.; Schmidt, S.; Morís, F.; Kroutil, W.; Gonzaíez-Sabín, J.; Kourist, R. Using Deep Eutectic Solvents to Overcome Limited Substrate Solubility in the Enzymatic   Decarboxylation   of   Bio-Based   Phenolic   Acids.   **2019**. https://doi.org/10.1021/acssuschemeng.9b03455.

(61)   MSDS   -   1613757 https://www.sigmaaldrich.com/MSDS/MSDS/DisplayMSDSPage.do?country=AT&language=de&productNumber=1613757&brand=USP&PageToGoToURL=https%3A%2F%2Fwww.sigmaaldrich.com%2Fcatalog%2Fsearch%3Fterm%3Dna2co3%26interface%3DAll%26N%3D0%26mode%3Dmatch%2520partialmax%26lang%3Dde%26region%3DAT%26focus%3Dproduct (accessed Dec 20, 2019).

(62)   k2co3 | Sigma-Aldrich https://www.sigmaaldrich.com/catalog/search?term=k2co3&interface=All&N=0&mode=match partialmax&lang=de&region=AT&focus=product (accessed Dec 20, 2019).

(63)   para-Coumaric Acid https://www.drugbank.ca/drugs/DB04066 (accessed Dec 20, 2019).

(64)   Li, B.; Guan, Z.; Wang, W.; Yang, X.; Hu, J.; Tan, B.; Li, T. Highly Dispersed Pd Catalyst Locked in Knitting Aryl Network Polymers for Suzuki-Miyaura Coupling Reactions of Aryl Chlorides   in   Aqueous   Media.   *Adv.   Mater.*   **2012**,   *24*   (25),   3390–3395. https://doi.org/10.1002/adma.201200804.

(65)   Baidya, T.; Gupta, A.; Deshpandey, P. A.; Madras, G.; Hegde, M. S. High Oxygen Storage Capacity and High Rates of CO Oxidation and NO Reduction Catalytic Properties of Ce 1-x Sn x O 2 and Ce 0.78 Sn 0.2 Pd 0.02 O 2-δ. https://doi.org/10.1021/jp8060569.

(66)   Lichtenegger, G. J.; Maier, M.; Hackl, M.; Khinast, J. G.; Gössler, W.; Griesser, T.; Kumar, V. S. P.; Gruber-Woelfler, H.; Deshpande, P. A. Suzuki-Miyaura Coupling Reactions Using Novel Metal Oxide Supported Ionic Palladium Catalysts. *J. Mol. Catal. A Chem.* **2017**, *426*, 39–51. https://doi.org/10.1016/j.molcata.2016.10.033.